OUKA
Osaka University Knowledge Archive

Title	STUDIES ON MESOMORPHIC AND PHOTOCONDUCTIVE PROPERTIES OF SEVERAL COMPOUNDS CONTAINIG HETEROAROMATIC MOIETIES
Author(s)	Shimizu, Yo
Citation	大阪大学, 1986, 博士論文
Version Type	VoR
URL	https://hdl.handle.net/11094/357
rights	
Note	

Osaka University Knowledge Archive : OUKA

https://ir.library.osaka-u.ac.jp/

Osaka University

STUDIES ON MESOMORPHIC AND PHOTOCONDUCTIVE PROPERTIES OF SEVERAL COMPOUNDS CONTAINING HETEROAROMATIC MOIETIES

1986

YO SHIMIZU

STUDIES ON MESOMORPHIC AND PHOTOCONDUCTIVE PROPERTIES OF SEVERAL COMPOUNDS CONTAINING HETEROAROMATIC MOIETIES

(複素芳香環を含む化合物の液晶性及び光電導性に関する研究)

1986

YO SHIMIZU

Preface

The works of this thesis were carried out under the guidance of Professor Shigekazu Kusabayashi at Faculty of Engineering, Osaka University.

The aim of this thesis is to study the mesomorphic properties of molecules containing heteroaromatic moieties in search of new liquid crystals possessing some functions.

Yo Shimizu

Faculty of Engineering,
Osaka University,
Yamada-oka, Suita,
Osaka 565,
Japan

January, 1986

List of Papers

1) Novel Smectic C Mesogens. 3-(2-Hydroxy-4-alkoxybenzylideneamino)-dibenzofurans

Y. Shimizu and S. Kusabayashi, Chem. Lett., 1003(1985).

2) Occurrence of the Smectic C Phase for 3-(2-Hydroxy-4-alkoxybenzylideneamino)dibenzofurans

Y. Shimizu and S. Kusabayashi, Mol.Cryst.Liq.Cryst., in press.

3) Mesomorphic Thermal Stability of 3-(4-Alkoxybenzylideneamino)dibenzofurans and 3-(4-Alkoxybenzylideneamino)dibenzothiophenes

Y. Shimizu, A. Ikegami, M. Nojima and S. Kusabayashi, Mol.Cryst.Liq.Cryst., in press.

4) A N-S_A-S_C-S_A Reentrant Phenomenon by a Binary Mixture of Dodecyloxy and Tridecyloxy Homologues of 2-(4-Alkoxybenzylideneamino)fluorenones

Y. Shimizu and S. Kusabayashi, Mol.Cryst.Liq.Cryst.Lett., in press.

5) Mesomorphic Behaviors of 2-(2-Hydroxy-4-alkoxybenzylideneamino)-fluorenones

Y. Shimizu and S. Kusabayashi, J.Chem.Soc. Perkin 2, in preparation.

6) Mesomorphic and Photoconducting Behaviors of 2-(2-Hydroxy-4-alkoxybenzylideneamino)-9-methylcarbazoles

Y. Shimizu, K. Shigeta and S. Kusabayashi, Mol.Cryst.Liq.Cryst., in preparation.

7) Photoconducting Behaviors through Phase Transitions: 5,10,15,20-Tetrakis-(4-pentadecylphenyl)porphyrin

Y. Shimizu, A. Ishikawa and S. Kusabayashi, Chem.Lett., in preparation.

8) Phase Transition Behaviors of 5,10,15,20-Tetrakis(4-alkylphenyl)-porphyrins

Y. Shimizu, A. Ishikawa and S. Kusabayashi, J.Chem.Soc. Perkin 2, in preparation.

CONTENTS

GENERAL INTRODUCTION

States of matters could be regarded as the assembly of molecules under the appropriate conditions of temperature and pressure. This means a "thermotropic" phase. Before 1888, it must have been believed that we have only three phases in the natural world ——— solid, liquid and gaseous phases. Considering the classification of states, however, why did no one expect a possibility of the intermediate states among them? and didn't they wonder that nature is so discontinuous as such in the phenomenal sense?

It was in 1888 that one answer to those doubts was first found by F.Reinitzer, a Austrian botanist.[1] He noticed the white-turbid molten state between the transparent liquid and the crystalline phase as the temperature was elevated. After that, this state was revealed to be the state with some kinds of molecular ordering like a crystal, but with fluidity like a liquid, what is called "liquid crystals".[2]

There has been past about a century since then and the liquid crystals have been reached to the magnificent application to the display devices.[3]

In a true sense, it is in a few decades that the studies of liquid crystals became extensive and have been extended to such fields for many aspects, as not only the material science but also the nature of mesophases itself.

A term "mesophase" means an intermediate phase. In addition to liquid crystals, "plastic crystals" also are classified into mesophases, which are occasionally found in the spherical shaped

molecules like adamantane.[4] Plastic crystals were discovered first by J.Timmermanns in 1935.[5]

From a viewpoint of molecular shapes, rod-like liquid crystals are of one-dimention and spherical plastic crystals are of three-dimention. Then it is reasonable to think, based on a beauty of nature in a symmetrical sense, that some kinds of two-dimentional molecules must show mesophases, what became to be called later "discotic liquid crystals". Discotic mesophases were first found for a benzene hexa-n-alkanoate in 1977 by S.Chandrasekhar et al.[6]

Therefore, we have three types of mesogens in the natural world, depending on the molecular shapes. And furthermore, each type of these mesogens has some variations of the phases exhibited, except that plastic crystals have not been found in the variations of mesomorphic structures.

Nowadays, the rod-like liquid crystals have two kinds of mesophases, nematic and smectic phases, in which molecules align in the parallel direction along the long axis without forming layer and with layered structures, respectively, as shown in Scheme I. Moreover, the smectic phases could be divided into eleven classes depending on the alignment within the layer. We name them to be "smectic A, smectic B, smectic C,.....,smectic K" except for smectic D phase being cubic.[7]

On the other hand, the disk-like(discotic) liquid crystals also have two kinds of mesomorphic structures on the whole. The one is with molecular alignment in the parallel direction of a molecular plane and wiyhout correlation of the alignment in the perpendicular to the plane, and the other is stacked columnar phases as illustrated in Scheme II. Furthermore, the

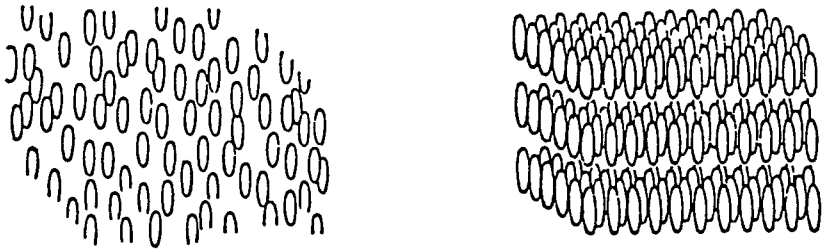

(a) (b)

Scheme I Schematic representations of molecular alignments of rod-like liquid crystals in (a) nematic and (b) smectic phases.

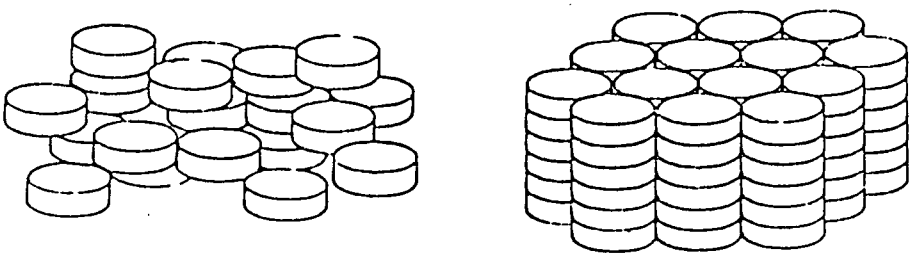

(a) (b)

Scheme II Schematic representations of molecular alignments of disk-like (discotic) liquid crystals in (a) discotic nematic and (b) stacked columnar phases.

columnar phases could be classified into several types of the columnar structure, now we have five classifications about them.[8]

At present, the rod-like liquid crystals have been focussed on the industrial technology, the new flat display devices instead of CRT displays in the near future. On the discotic liquid crystals, however, no possibility of the application has been found as in the same situation of the plastic crystals.

By the way, to the display devices using rod-like liquid crystals, though only the nematic phase is used actually, simply are applied the function that the molecular alignment could be

changed by the electric field. The properties of the molecules themselves are not considered in an available way. This recognition could be the next step for the further advance of liquid crystals with some kinds of functions, meaning that the combination of the molecular intrinsic properties with the switching function having been used so far, could be the next target.

According to such senses, some rod-like liquid crystals containing a heteroaromatic moiety and 5,10,15,20-tetraphenylporphyrins with long aliphatic chains as seen in Scheme III, are paid attention to this work.

At the beggining, those compounds were investigated on the

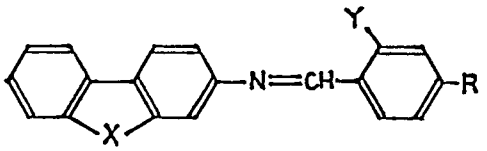

1; Y=H, R=$OCH_2(CH_2)_{n-2}CH_3$
2; Y=OH, R=$OCH_2(CH_2)_{n-2}CH_3$
3; Y=H, R=$CH_2(CH_2)_{n-2}CH_3$

a; X= — O —
b; X= — S —
c; X= — CH_2 —
d; X= — CO —
e; X= — $N(CH_3)$ —

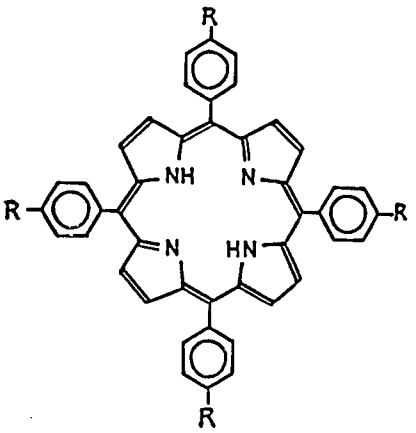

4

a; R=$CH_2(CH_2)_{n-2}CH_3$
b; R=$OCH_2(CH_2)_{n-2}CH_3$

Scheme III Compounds investigated on the mesomorphic and photoconductive behaviors in this work.

mesomorphic properties, which are described in chapter I and II for rod-like and disk-like compounds, respectively. Furthermore, the photoconductive properties were investigated mainly from a viewpoint of phase transitions, described in chapter III.

REFERENCES

1) F.Reinitzer, Mh.Chem., 9, 421(1888).

2) O.Lehmann, Z.Phys.Chem., 4, 462(1889).

3) M.Okano and S.Kobayashi ed., "Liquid Crystals", Baifukan, Tokyo, 1985.

4) G.W.Gray and P.A.Winsor ed., "Liquid Crystals & Plastic Crystals", Vol.1, John Wiley & sons, London, 1974.

5) J.Timmermanns, Bull.Soc.Chem.Belg., 44, 17(1935).

6) S.Chandrasekhar, B.K.Sadashiva and K.A.Suresh, Pramana, 9, 471(1977).

7) G.W.Gray and J.W.Goodby, "Smectic Liquid Crystals —— textures and structures", Leonard Hill, London, 1984.

8) J.C.Dubois and J.Billard, "Liquid Crystals and Ordered Fluid", Vol.4, 1043(1983).

CHAPTER I

Mesomorphic Behaviors of Benzylideneamino-heteroaromatics

I — 1 Mesomorphic thermal stability of 3-(4-alkoxybenzylideneamino)-dibenzofurans and 3-(4-alkoxybenzylideneamino)dibenzothiophenes

The liquid crystalline properties of Schiff's base compounds (I) containing fluorene(I,X=—CH_2—)[1], fluorenone(I,X=—CO—)[1], 9-methyl- and 9H-carbazoles(I,X=—N(CH_3)— and X=—NH—, respectively)[2], 9,10-dihydrophenanthrene(I,X=—CH_2CH_2—)[3], and phenanthrene(I,X=—CH=CH—)[4] have already been reported for their homologous series.

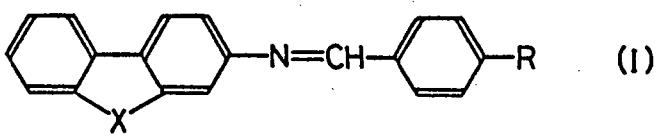

(I)

R=alkoxyl

The effect of a hetero atom(X) on the mesomorphic thermal stability has not so far been discussed.

In this section, the thermal stability of dibenzofuran and dibenzothiophene analogues(I,X=—O— and X=—S—, respectively) were studied from the viewpoints of the molecular geometry and the polarizability.

The transition temperatures and enthalpies of 3-(4-alkoxybenzylideneamino)dibenzofurans(1a) and 3-(4-alkoxybenzylideneamino)dibenzothiophenes(1b) are shown in Table I and II. Figures 1 and 2 show the mesomorphic trends of each homologous series.

In both cases of 1a and 1b, the mesomorphic trends are

similar to those of the other liquid crystals(I) in the odd-even alternation of the nematic to isotropic phase transition temperatures, the appearance of the smectic A phase in the region of the longer alkyl chain($n \geq 7$), and the disappearance of the nematic phase in the longer homologues.

Table I

Transition temperatures and enthalpies of 3-(4-alkoxybenzylideneamino)dibenzofurans(1a)

n	$T_{C-S_A,N \text{ or } I}$	$\Delta H_{C-S_A,N \text{ or } I}$	$T_{S_A-N \text{ or } I}$	$\Delta H_{S_A-N \text{ or } I}$	T_{N-I}	ΔH_{N-I}
1	150.5	35.2				
2	129.5	30.2			167.5	0.7
3	133.5	35.6			146.5	0.4
4	124.5	24.7			158.5	0.5
5	115.5	34.4			148.5	0.5
6	112.5	29.7			154.5	0.5
7	113.5	34.2	115.5	0.7	150.5	0.3
8	118.5	38.4	128.5	5.1	152.5	0.4
9	116.2	50.2	132.5	1.9	149.6	0.8
10	113.5	51.4	136.5	2.3	148.6	1.1
11	117.4	61.5	139.0	2.7	146.3	1.0
12	120.4	57.3	140.6	3.5	145.0	1.6
14	116.2	66.5	139.7	3.7	140.5	2.2

[a] T in °C and ΔH in kJ/mol.

Table II

Transition temperatures and enthalpies of 3-(4-alkoxybenzylideneamino)dibenzothiophenes(1b)

n	$T_{C-S_A \text{ or } N}$	$\Delta H_{C-S_A \text{ or } N}$	T_{S_A-N}	ΔH_{S_A-N}	T_{N-I}	ΔH_{N-I}
5	130.5	43.6			174.9	0.7
6	123.3	42.3			177.6	1.0
7	117.4	28.8	[107.8][b]	0.2	170.2	1.0
8	115.0	28.3	119.4	0.6	170.0	1.2
9	112.3	29.9	128.2	1.0	164.6	1.2
10	109.6	27.4	135.4	1.4	163.5	1.3

[a] T in °C and ΔH in kJ/mol.
[b] [ ]: monotropic transition.

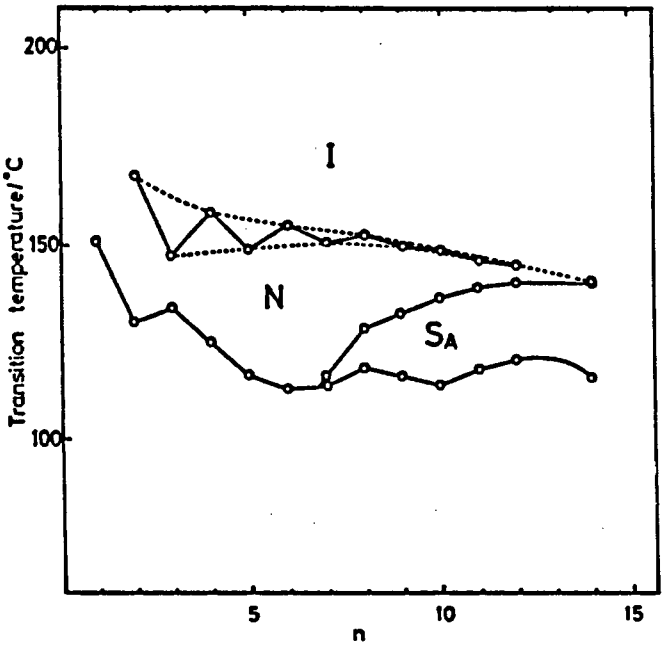

Figure 1 Plots of transition temperatures against the number of carbon atoms(n) in the alkyl chain of 3-(4-alkoxybenzylideneamino)dibenzofurans(1a).

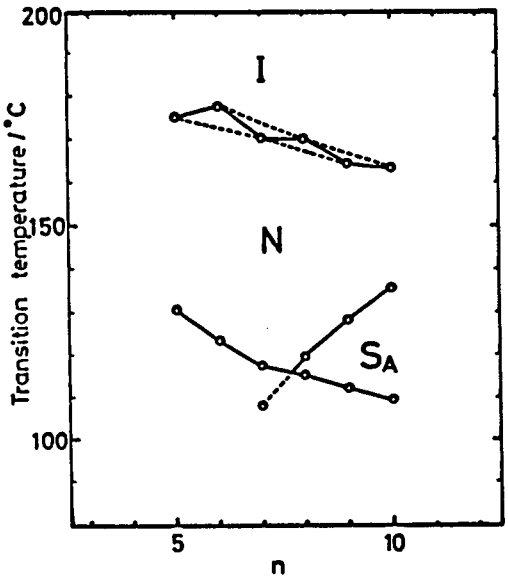

Figure 2 Plots of transition temperatures against the number of carbon atoms(n) in the alkyl chain of 3-(4-alkoxybenzylideneamino)dibenzothiophenes(1b).

In order to compare the mesomorphic thermal stability of 1a with that of 1b, the average values of the nematic to isotropic phase transition temperatures(T_{NI}) from heptyloxy to decyloxy derivatives were calculated as follows:

	1a	1b
T_{NI}	150.3°C	167.1°C

The averaged T_{NI} of 1a is lower by 16.8° than that of 1b.

The degree of the molecular interaction would be determined by the intermolecular separation and the polarizability anisotropy(Eq. 1).[5] Therefore, an effective molecular volume

$$T_{NI} = \frac{2(\Delta\alpha)^2}{4.54k - 2A} \qquad \text{--------(1)}$$

k; Boltzmann constant.

$\Delta\alpha$; the anisotropy of the molecular polarizability.

A; the term in relation to the effective length/ width ratio of the molecule.

due to the rotation about the molecular long axis would be crucial for the intermolecular force. Hence, the molecular planarity and the molecular width are important factors for the mesomorphic thermal stability(T_{NI}). Thus, it is worthwhile to investigate the conformation of these compounds from the viewpoint of the molecular volume as well as the polarizability anisotropy, which seems to be affected by the degree of the conjugation of π-electrons.

It is generally considered that diarylazomethine is not

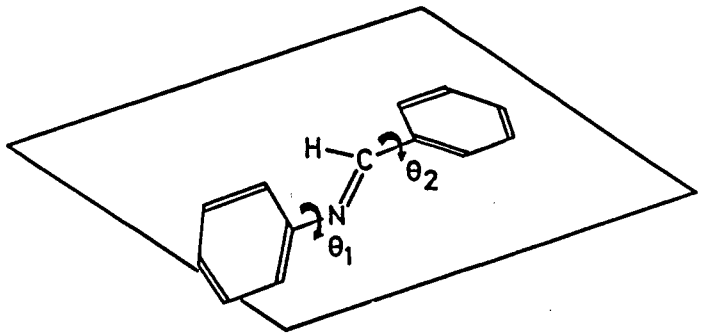

Figure 3 Twisted conformation of N-benzylideneaniline.

a co-planar molecule as seen in Figure 3. For example, N-benzylideneaniline[BA] has the twist angles θ_1 about the Ar-N= bond and θ_2 about the Ar-C= bond. In a crystalline state, θ_1= 55° and θ_2=-10.3° have been reported.[6]

In order to estimate the twist angles θ_1 of 1a and 1b, the UV absorption spectra were measured to give the results in Table III.

The band having λ_{max}340-370nm seems to be assigned to the π-π^* transition band which is due to the conjugation of the heteroaromatic group to the benzylideneamino moiety.[7] This assignment could be supported by a decreased ε_{max} of the longest wavelength band[7,8] of 3-(α-methyl-4-pentylbenzylideneamino)dibenzofuran[DBFC5Me], which seems to have a larger twist angle θ_1 because of the steric hindrance of α-methyl group against the 2- and 4-site protons of dibenzofuran. The absorption coefficients of those bands could be used for a rough estimate of θ_1 by the following equation(Eq. 2);[9]

$$\cos^2\theta_1 = \varepsilon_1 / \varepsilon_0 \qquad \text{----------(2)}$$

where ε_1 is the absorption coefficient of the molecule with

Compound	λ_{max}/nm	ε_{max}	θ_1 /°[b]
BA	310(310)[c]	8400(7000)	46(50)
SA	339(340)	11800(11200)	35(35)
DBFOC5 (1a)	343	27400	43
DBFC5Me	ca.340[d]	7400	68
DBFOC5Hy (2a)	358	34300	35
DBTOC5 (1b)	340	28500	43
DBTOC5Hy (2b)	358	35200	35
FLOC5[e] (1c)	347	27000	42
FLOC5Hy[f] (2c)	361	33200	35

a) All measurements were carried out at room temperature.
b) Calculated values by the equation: $\cos^2\theta_1 = \varepsilon_1/\varepsilon_0$.
c) Values in parenthesis are the reported ones (in cyclohexane), except for the θ_1 which were calculated with the equation above.
d) Appeared to be a shoulder band.
e) FLOC5: 2-(4-pentyloxybenzylideneamino) fluorene
f) FLOC5Hy: 2-(2-hydroxy-4-pentyloxybenzylideneamino) fluorene

Table III (left) Results of UV-absorption spectra in $CHCl_3$.[a]

Compound	Chemical Shift /ppm δ_a	δ_b	δ_c	$\Delta\delta_c$	δ_d
Aniline	6.45		—	—	—
BA	6.9 — 7.3		8.27	0.30	b)
SA	6.7 — 7.5		8.57		b)
3ADBF	6.79	6.65	—	—	—
DBFC5Me	6.95	6.77	—	—	b)
DBFOC5 (1a)	7.1 — 7.5		8.42	0.14	7.83
DBFOC5Hy (2a)	7.1 — 7.5		8.56		b)
3ADBT	6.96	6.67	—	—	—
DBTOC5 (1b)	7.2 — 7.7		8.45	0.13	7.84
DBTOC5Hy (2b)	7.2 — 7.7		8.58		b)
2AFL[c]	6.75	6.61	—	—	—
FLOC5 (1c)	7.1 — 7.5		8.43	0.12	7.80
FLOC5Hy (2c)	7.1 — 7.5		8.55		b)

a) In $CHCl_3$ at room temperature. TMS was used as internal standard.
b) The assignments could not be carried out.
c) 2AFL: 2-aminofluorene

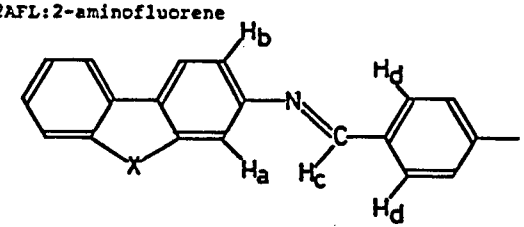

Table IV (right) Results of ^{1}H-NMR spectra.[a]

the twist angle θ_1 and ε_0 is the absorption coefficient of its planar analogue.

The application of the Eq. 2 to the results by P.Skrabal et al.[8] leads to θ_1=50° for BA in cyclohexane. This estimated value for BA agrees well with the results of X-ray analysis[6] and theoretical calculations[8,10]. Salicylideneaniline[SA] has ε_{max}(λ_{max}=340nm) of 11200 in cyclohexane and its θ_1 is calculated to be 35°. The absorption spectra of BA and SA in chloroform have respectively little change for the ε_{max} and λ_{max} as compared with those in cyclohexane.

This result would be reasonable considering that the intramolecular hydrogen bonding between 2-hydroxyl group and nitrogen lone pair electrons in azomethine linkage could destabilize the twist conformation to make the molecule more planar.[10]

The results of ^{1}H-NMR spectra show that the twist angles θ_1 are comparable to each other in SA, 3-(2-hydroxy-4-pentyloxybenzylideneamino)dibenzofuran(2a;n=5) and 3-(2-hydroxy-4-pentyloxybenzylideneamino)dibenzothiophene(2b;n=5), since δ_C for these molecules are almost the same as shown in Table IV. Thus, the twist angles θ_1 for 2a and 2b are considered to be almost the same to each other(about 35°).

The twist angles θ_1 of the others were estimated with the Eq. 2 and the ε_0 were calculated back from the value θ_1 of the 2-hydroxy derivatives.

The estimated twist angles θ_1 are comparable to each other in 1a(n=5) and 1b(n=5). This result is also supported by the results of ^{1}H-NMR chemical shifts.

The twist angle θ_1 could influence the environment of

the two ortho-site protons of dibenzofuran and dibenzothiophene(H_a and H_b) and the α-site proton of benzylidene moiety (H_c).

The chemical shift gaps $\Delta\delta_c$ are 0.14ppm for 1a and 2a, and 0.12ppm for 1b and 2b. This indicates that the twist angles θ_1 are almost the same in 1a and 1b. The $\Delta\delta_c$ for BA and SA(0,30ppm) indicates that BA has a larger twist angle θ_1 than 1a and 1b, and this result agrees with the results of UV absorption spectra. As for the δ_a and δ_b, the detailed analysis was difficult to be carried out, as these chemical shifts are shadowed by the other aromatic protons' multiplet signals. Compared with the relation between aniline and BA, however, the gaps between 3-aminodibenzofuran[3ADBF] and 1a, and 3-aminodibenzothiophene[3ADBT] and 1b in δ_a and δ_b, seem to indicate that θ_1 for 1a and 1b are smaller than that of BA, as the chemical shift of the two protons are considered to shift to a higher field when the twist angle increases. In fact, the δ_a and δ_b for DBFC5Me are 6.95 and 6.77ppm, respectively and higher than those of 1a and lower than those of 3ADBF.

On the other hand, the twist angles θ_2 for 1a and 1b seem to be comparable to each other because of the similar values of their δ_d.

Thus, the conformations for 1a and 1b are comparable to each other. This relation of their conformations does not seem to change in mesophases in which molecules could rotate freely about their long axis. Therefore, the effects of their conformation on the effective molecular volume and the molecular polarizability are considered to be almost the same for 1a and 1b.

The molecular width, however, is also an important factor for the mesomorphic thermal stability(T_{NI}). This factor seems to affect the effective molecular volume.

The bond angle ϕ of (II), which is assumed to be the same as that of (I), seems to be crucial for the determination of the molecular width, since the rotation about Ar-N= bond occurs in mesomorphic states as shown in Figure 4. The width decreases as the value of ϕ approaches to 120° and the narrow width leads to a decrease in the molecular effective volume.

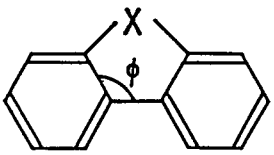

(II)

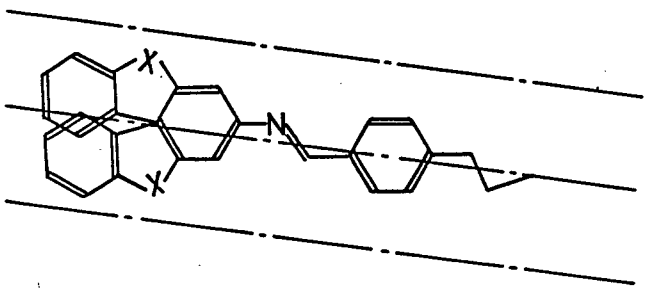

Figure 4 Bond angle ϕ and effective molecular volume determined by the ϕ-value.

According to the crystal structures by X-ray analyses, the bond angles ϕ of dibenzofuran and dibenzothiophene are 105.6°[11] or 106.3°[12] and 111.4° or 112.4°[13], respectively. Thus, the width decreases in the following order:

dibenzofuran > dibenzothiophene

This indicates the thermal stability of mesophases tends to increase in this order:

dibenzofuran < dibenzothiophene

The order agrees with that of T_{NI} in 1a and 1b.

K.J.Miller et al. reported an empirical method for calculating average molecular polarizability.[14] According to the calculation method, the average molecular polarizabilities of dibenzofuran and dibenzothiophene could be estimated to be 19.93 and 22.32A^3, respectively. The anisotropy of the molecular polarizability seems to be the same order as the average molecular polarizability because of the same order of the optical anisotropy for dibenzofuran and dibenzothiophene.[15] These orders also agree with that of T_{NI} in 1a and 1b.

Therefore, the order of the mesomorphic thermal stability of 1a and 1b could be explained in terms of the molecular polarizability(anisotropy) and the molecular width. These results indicate that the bridging atom(X) in the heteroaromatic ring could significantly affect the mesomorphic thermal stability.

However, 2-(4-alkoxybenzylideneamino)fluorenes(1c), the structural analogues to 1a and 1b, have higher T_{NI} than those of 1a and 1b. The averaged T_{NI} in heptyloxy to decyloxy derivatives is 186.4°C.[1]

The average molecular polarizability for fluorene was reported to be 21.15A^3 [14] and the optical anisotropy was measured to be smaller than those of dibenzofuran and dibenzothiophene.[15] This seems to indicate that the mesomorphic thermal stability of 1c could not be explained only by the polarizability. The

width is not significantly different from those of dibenzofuran and dibenzothiophene. The ϕ-value for fluorene is reported to be 107.6°[16] or 108°[17]. The conformation of 1c estimated by the method described above seems to be almost the same as those of 1a and 1b, as shown in Table III and IV. These results might indicate the possibility of the existence of other factors which determine the mesomorphic thermal stability for these kinds of mesogens.

Conclusion

The homologous series of 3-(4-alkoxybenzylideneamino)dibenzofurans and 3-(4-alkoxybenzylideneamino)dibenzothiophenes were prepared and their mesomorphic behaviors were revealed. Some factors determined the mesomorphic thermal stability were examined and the results indicate that the bridging atom(X) incorporated in the structure(I) significantly affects the mesomorphic thermal stability.

I — 2 A relation of the structural factors of molecules and the transverse dipoles for the occurrence of the smectic C phase in benzylideneamino-heteroaromatics

Many studies have so far been made of the structure and the formation of the smectic C phase, and the structure was revealed to be analogous to that of the smectic A phase except for its tilt alignment to the layer normal.[18] Though many factors have been proposed for the occurrence of the smectic C phase, it seems that no definite conclusion has been reached yet.

W.L.McMillan proposed that, due to structural factors for the occurrence of the smectic C phase, the molecule should have an approximate center of symmetry, large outboard(antiparallel) dipole moments and a zig-zag(trans) gross shape as shown in scheme below.[19] A.Wulf also proposed the steric model for the

McMillan's model

- approximately symmetrical molecular structure
- terminal outboard dipole moment
- freezed-out rotation

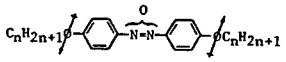

driving force of the tilt alignment, assuming that the molecule is symmetrical and zig-zag shaped.[20]

Wulf 's steric model

- zig-zag shaped molecules

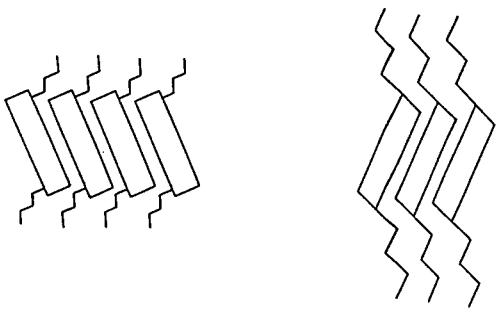

On the other hand, experimental results which do not agree with the above theories have been reported. J.W.Goodby et al. have illustrated that the lack of one-side dipole of the two outboard ones does not lead to the disappearance of the smectic C phase, and that branching in the terminal alkyl chain also does not lead to the vanishing of the smectic C phase.[21]

At present, it has been accepted that the favorable factors for the occurrence of the smectic C phase are (1)the approximately symmetrical molecular structure, (2)two alkyl chains at both ends of the core moiety, (3)the appropriate length of the terminal alkyl chain and (4)terminal outboard dipole moments.[18]

However, it was found 3-(2-hydroxy-4-alkoxybenzylideneamino)dibenzofurans(2a) are smectic C mesogens with pentyloxy to dodecyloxy terminal chains.

In order to study the relation of molecular geometry and molecular dipoles to the occurrence of the smectic C phase, the geometrical analogues to 2a were prepared and their mesomorphic behaviors were investigated.

The mesomorphic behavior of 2a shows the normal trend for the nematic and smectic A phases. As seen in Figure 5(the transition temperatures were listed in Table V.), the nematic to isotropic transition temperatures show a normal odd-even alternation and the smectic A to nematic transition temperatures gradually rise as the terminal alkyl chain length increases, leading to the disappearance of the nematic phase in the higher members of the homologous series.

The smectic C phase of 2a appeared in pentyloxy to dodecyl-

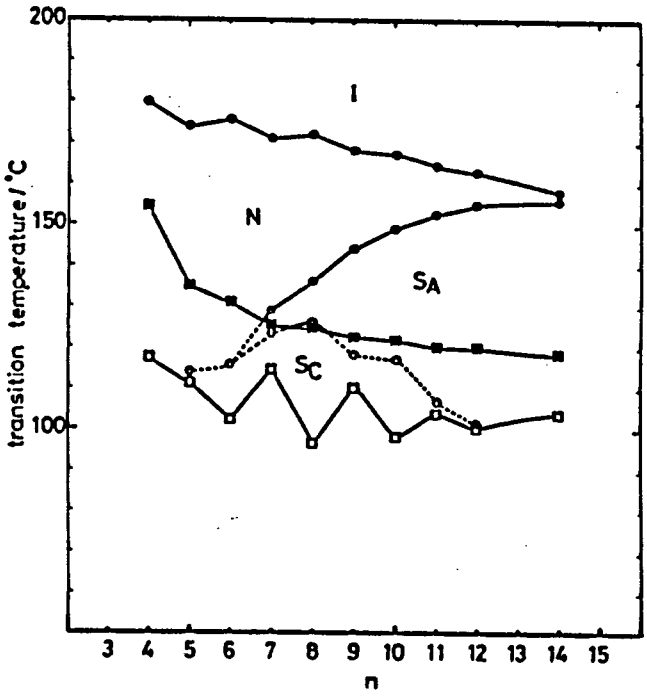

Figure 5 Plots of transition temperatures against the number of carbon atoms(n) in the alkyl chain of 3-(2-hydroxy-4-alkoxybenzylideneamino)dibenzofurans(2a). ■;melting point and □;crystallization on cooling at 5°C/min.

Table V

Phase transition temperatures(T/°C) of 3-(2-hydroxy-4-alkoxybenzylideneamino)dibenzofurans(2a)

n	$T_{C\text{-}S_C,S_A \text{ or } N}$	$T_{S_C\text{-}S_A \text{ or } N}$	$T_{S_A\text{-}N \text{ or } I}$	$T_{N\text{-}I}$	$T_{rec.}$[a]
4	154.5			179.6	117.5
5	135.0	(113.9)[b]		173.9	111.2
6	131.1	(115.7)		175.6	102.5
7	125.6	(123.5)	128.0	171.1	114.6
8	124.8	125.8	136.2	172.0	96.5
9	122.6	(118.4)	144.3	168.3	110.4
10	121.8	(117.3)	149.2	167.6	98.5
11	120.1	(106.6)	152.5	164.3	104.1
12	119.8	(101.6)	154.8	162.7	100.5
14	118.6		156.0	158.1	104.0

[a] C:crystal, S_C:smectic C, S_A:smectic A, N:nematic, I:isotropic and rec.:recrystallization (cooling rate:5°C/min.).

[b] ( ):monotropic transition.

oxy derivatives as a monotropic transition except for an enantiotropic octyloxy derivative. The curve of the smectic C to nematic or to smectic A transition temperatures against the number of carbon atoms in the alkyl chain is "parabolic", as G.W.Gray et al. referred to,[22] but is a broader one and reaches maximum with an octyloxy compound. The odd-even alternation of the transition temperatures is ambiguous as compared with that of the biphenyl derivatives having two alkyl chains (5a and 5b).[22]

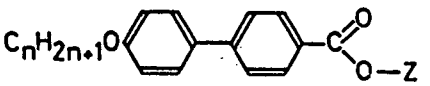

(5)

a; Z = $-C_nH_{2n+1}$. b; Z = 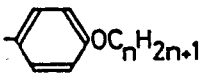

This smectic C phase was identified by the miscibility test with terephthalylidene-bis(butylaniline) [TBBA][23], as shown in Figure 6.

The microscopic observations of the smectic C phase exhibited two kinds of textures("Schlieren" and "broken fan" in the homeotropic and homogeneous parts of the smectic A phase on cooling, respectively.). However, the smectic C to smectic A transition could not be detected by DSC measurement, probably <0.01kJ/mol., indicating that it is a second-order or a weak first-order phase transition.

The smectic C mesogens 2a, are not symmetrical and has only one terminal alkyl chain. Furthermore, it has no terminal outboard dipole moment. A terminal dipole of the alkoxyl group would not be regarded as "outboard" one owing to the absence of the counter dipole at the end of dibenzofuran core.

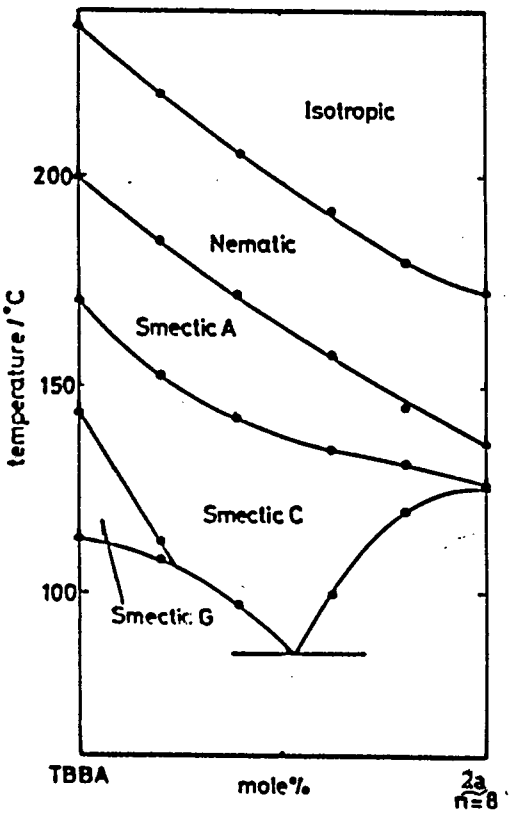

Figure 6

A miscibility diagram between 2a(n=8) and TBBA.

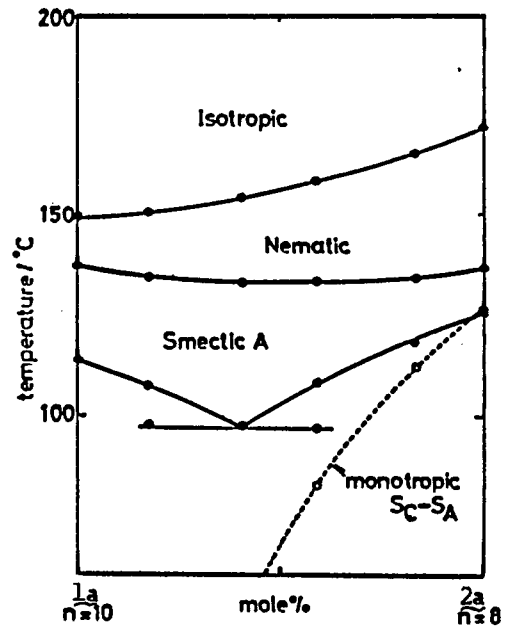

Figure 7

A binary phase diagram of 2a(n=8) and 1a(n=10).

A comparison with 3-(4-alkoxybenzylideneamino)dibenzofurans(1a) indicates that the additional hydroxyl group raises the mesomorphic thermal stability by about 30°C and that the mesomorphic temperature range is enlarged by about 10°, while the addition does not change the behaviors of the nematic and smectic A phases in relation to the length of the alkyl chain with regard to the appearance of the smectic A phase and the disappearance of the nematic phase.

Furthermore, it is evident that the lateral hydroxyl group enhances the smectic C thermal stability, leading to the injection of the smectic C phase underlying the smectic A and nematic phases, since the miscibility test indicated that the thermal stability of the smectic C phase(the virtual transition temperatures $T_{S_C-S_A}$) in 1a seems to be very low, inferred from Figure 7.

On the other hand, though the mesomorphic behaviors of 2-(4-alkoxybenzylideneamino)fluorenones(1d) were firstly reported in 1955 by G.W.Gray et al., they could classify the two mesophases to be nematic and smectic ones at that time.[1] In 1974, G.W.Gray et al. themselves reexamined the hexadecyloxy derivative to have nematic and smectic A phases.[24] However, G.Sigaud et al. reported that the heptyloxy derivative shows no smectic A phase but smectic C phase in addition to the nematic phase.[25] Therefore, the interesting liquid crystals 1d were reinvestigated on the mesomorphic behaviors for the homologous series. The mesomorphic trend is shown in Figure 8 and the transition temperatures were listed in Table VI.

The fluorenone liquid crystals 1d are smectic C mesogens. The smectic phase between n=6 and n=11 is smectic C phase.

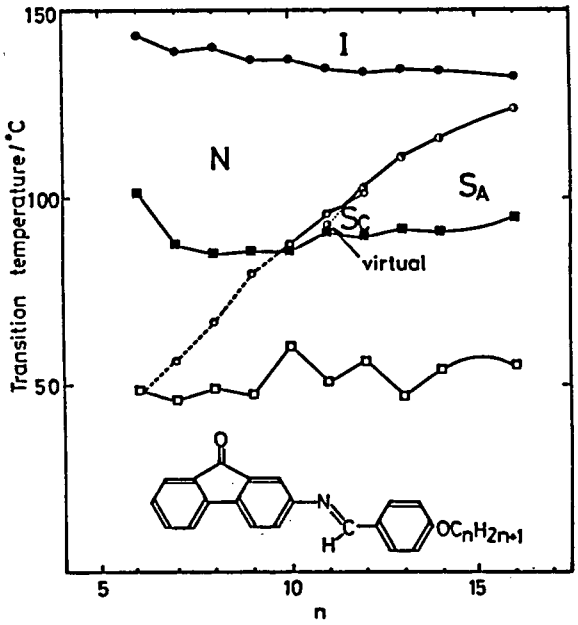

Figure 8 Plots of transition temperatures against the number of carbon atoms(n) in the alkyl chain of 2-(4-alkoxybenzylideneamino)fluorenones(1d). ●;N-I, ◐;S_A-N, ○;S_C-S_A or N and ■;melting point and □;crystallization on cooling at 5°C/min.

Table VI

Phase transition temperatures(T/°C) of 2-(4-alkoxybenzylideneamino)fluorenones(1d)

n	$T_{C-S_C,S_A \text{ or } N}$	$T_{S_C-S_A \text{ or } N}$	T_{S_A-N}	T_{N-I}	$T_{rec.}$ [a]
6	101.5			143.5	48.5
7	87.7	[56.5] [b]		138.9	46.0
8	85.2	[67.2]		140.2	49.0
9	86.0	[80.0]		137.7	47.6
10	85.8	87.7		137.0	60.3
11	90.8	96.1		134.5	51.2
12	89.7	101.5	103.0	133.1	56.7
13	91.8		111.0	134.4	47.0
14	91.3		115.7	133.9	54.1
16	94.9		124.3	132.6	55.6

a) C:crystal, S_C:smectic C, S_A:smectic A, N:nematic, I:isotropic and rec.:recrystallization(cooling rate:5°C/min.).

b) [ ]: monotropic transition temperatures.

At n=12, 1d has smectic A phase in addition to the smectic C phase. However, in the longer alkyl chain length than n=13, the smectic C phase suddenly disappears and only the smectic A phase appears as a layer-structured phase.

The trend of the smectic phase(A and C) for the homologous series is normal in the viewpoint of the increase of the smectic thermal stability with the elongation of the terminal alkyl chain. The binary phase diagram between the undecyloxy and the dodecyl derivatives indicates the thermal stability of the smectic A phase underlies that of the smectic C phase in the undecyloxy derivative as shown in Figure 18(p.40). As a layered structure, that is, the smectic C structure is more stable than the smectic A structure in the shorter alkyl chain length than n=11. An inversion of the order of thermal stability for the smectic A and the smectic C phases occurs as passing from n=11 to n=12.

Furthermore, the binary phase diagram between the dodecyloxy and the tridecyloxy derivatives indicates that the latter has no ability to form a smectic C structure, inferred from Figure 19(p.43). This result reveals that the difference in the terminal alkyl chain length could be crucial for the ability to form the smectic C phase as a structural factors, for even the case that the difference is the length corresponding to only one carbon atom in the terminal alkyl chain.

On the other hand, the ortho-hydroxyl compounds of 1d, that is 2-(2-hydroxy-4-alkoxybenzylideneamino)fluorenones(2d), show the same trend in the homologous behaviors of the smectic C phase as 1d, except for that in the longer alkyl chain length

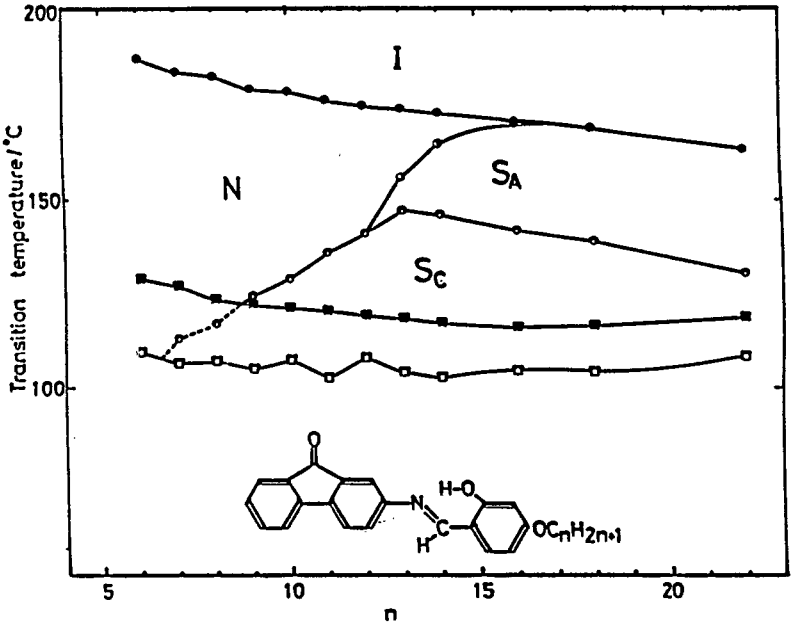

Figure 9 Plots of transition temperatures against the number of carbon atoms(n) in the alkyl chain of 2-(2-hydroxy-4-alkoxybenzylideneamino)fluorenones(2d). ●; N or S_A-I, ◐;S_A-N, ○;S_C-S_A or N, ■;melting point and □;crystallization on cooling at 5°C/min.

Table VII

Phase transition temperatures(T/°C) of 2-(2-hydroxy-4-alkoxybenzylideneamino)fluorenones(2d)

n	$T_{C-S_C \text{ or } N}$	$T_{S_C-S_A \text{ or } N}$	$T_{S_A-N \text{ or } I}$	T_{N-I}	$T_{rec.}$[a]
6	128.8	[101.7][b]		186.7	109.6
7	127.2	[113.1]		183.3	106.7
8	123.7	[117.2]		182.3	107.1
9	122.5	124.4		178.7	105.3
10	121.4	129.1		178.1	107.4
11	120.6	135.8		175.9	102.3
12	119.5	141.1		174.6	108.1
13	118.7	147.1	155.6	173.7	104.3
14	117.5	146.2	164.4	172.5	102.7
16	116.3	141.7	169.2	170.0	104.5
18	116.6	139.0	168.6		104.3
22	119.0	130.7	163.0		108.3

a) C:crystal, S_C:smectic C, S_A:smectic A, N:nematic, I:isotropic and rec.:recrystallization(cooling rate:5°C/min.).

b) [ ]: momotropic transition temperatures.

than n=13, up to n=22 as shown in Figure 9. The transition temperatures of 2d were listed in Table VII.

In this case, the additional hydroxyl group raises not only the mesomorphic thermal stability(T_{NI}) but the smectic C thermal stability as compared with those of 1d. However, the degree of increasing the smectic C thermal stability is far smaller than that in dibenzofuran analogues 1a and 2a. This phenomenon seems to be due to the sufficiently large thermal stability of the smectic C phase of 1d. In other words, a central and lateral hydroxyl group is considered to have a smaller effect for elevating the smectic C thermal stability than a transverse dipole of the heteroaromatic moiety, which is positioned at near end of the core moiety, as discussed later.

Furthermore, the additional hydroxyl group seems to have an effect on the force of forming the smectic C structure, that is, the crucial negative effect of the terminal alkyl chain on the ability to form the smectic C structure as molecular assembly as seen in 1d is considered to be relaxed to some extent by the addition of a hydroxyl group at a near center part of the core moiety, leading to the occurrence of the smectic C phase for the tridecyloxy to docosyloxy derivatives in contrast to the non-hydroxyl compound 1d. The central hydroxyl group seems to have an effect to make the smectic C structure tight.

It is in contrast that there exists the difference in the behaviors about the occurrence of the smectic C phase between these fluorenone liquid crystals(1d and 2d) and dibenzofuran ones(1a and 2a).

The difference between the fluorenone and dibenzofuran

liquid crystals appears to be in the next two factors, that is, (1)the magnitude of dipole moments contributing to the transverse component for the molecular long axis, and (2)the bulkiness of the carbonyl moiety.

The bulkiness, however, would not be considered to be a favorable factor for the occurrence of the smectic C phase, since 2-(2-hydroxy-4-alkoxybenzylideneamino)-9-methylcarbazoles (2e), which contain a bulky methyl group in the carbazole moiety just like 2d, does not exhibit the smectic C phase, though the smectic A phase appears as the alkyl chain becomes longer as shown in Figure 10, and the binary phase diagram between 2e(n=8) and 2a(n=8) indicates the smectic C thermal stability of 2e is estimated to be far lower than that of 2d, in Figure 11. The transition temperatures of 2e are listed in Table VIII.

Figure 11, moreover, indicates that the smectic A phase is able to exist with the lower thermal stability than that of the crystalline phase for the octyloxy derivative of 2e. Therefore, 2e could have a layered structure, but a smectic C structure could not be constructed with a higher thermal stability. Furthermore, the layered structure of 2e is inferred to be assisted to considerable extent by the longer alkyl chain. Thus, the bulkiness of 9-methyl group seems to be more disadvantageous for forming a layered structure than that of the carbonyl moiety in fluorenone skeleton, that is, methyl group seems to be more bulky than that of a carbonyl group.

On the other hand, fluorenone has been reported to have a pretty larger dipole moment than that of dibenzofuran, as seen in Table IX.

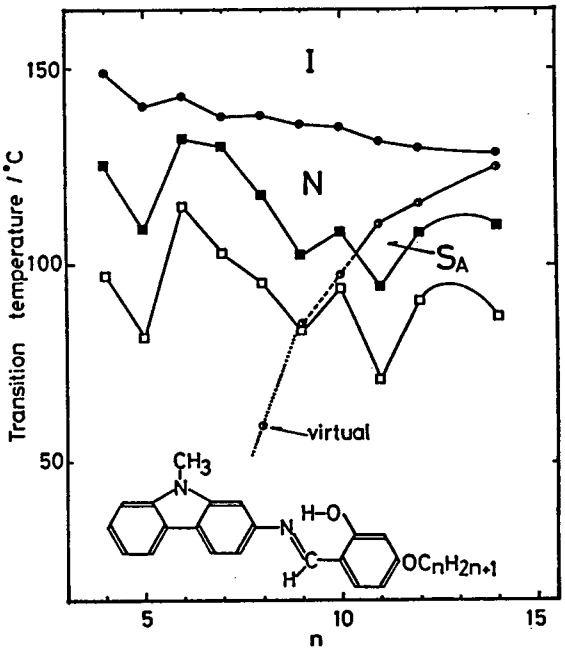

Figure 10 Plots of transition temperatures against the number of carbon atoms(n) in the alkyl chain of 2-(2-hydroxy-4-alkoxybenzylideneamino)-9-methylcarbazoles(2e). ●;N-I, ◐;S_A-N, ■;melting point and □;crystallization on cooling at 5°C/min.

Table VIII

Phase transition temperatures(T/°C) of 2-(2-hydroxy-4-alkoxybenzylideneamino)-9-methylcarbazoles(2e)

n	$T_{C-S_A \text{ or } N}$	T_{S_A-N}	T_{N-I}	$T_{cryst.}$ [a]
4	125.2		148.8	97.0
5	109.6		140.7	81.5
6	133.1		142.2	115.1
7	132.0		137.6	103.0
8	117.4		138.0	95.6
9	102.4	[85.0][b]	136.0	83.5
10	108.5	[97.5]	134.0	94.0
11	94.5	110.5	131.3	71.0
12	108.1	115.5	129.6	91.0
14	110.0	124.7	128.5	87.0

a) C:crystal, S_A:smectic A, N:nematic, I:isotropic and cryst.:crystallization on cooling at 5°C/min.

b) [ ]:monotropic transition.

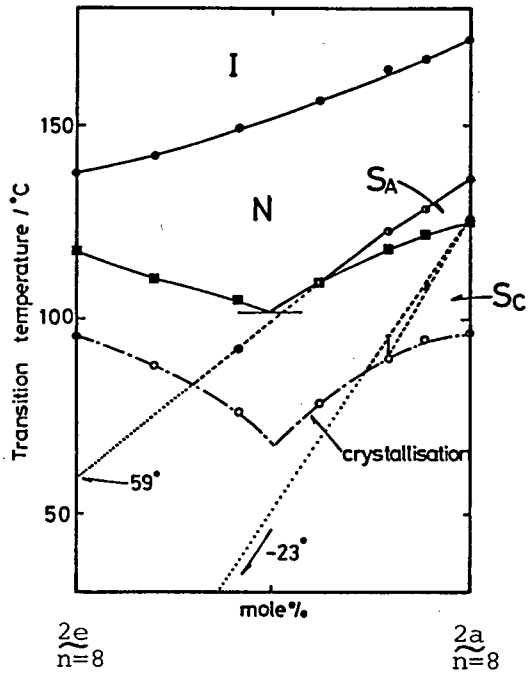

Figure 11

A binary phase diagram of 2e (n=8) and 2a (n=8).

DIPOLE MOMENTS of

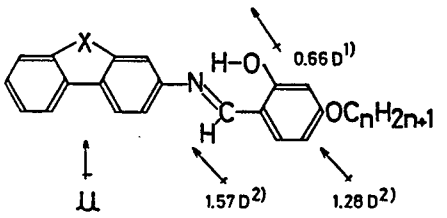

X	μ /Debye	ref.
—CH_2—	0.62	3)
—N(CH_3)—	0.66	4)
— S —	0.79	5)
— O —	0.82	5)
— CO —	3.36	5)

1) D.C.Colinese, J.Chem.Soc.(B), 857(1971).
2) R.T. Klingbiel et al., J. Am.Chem.Soc., 96, 7651(1974).
3) V. Baliah et al., Ind.J.Chem., 9, 563(1971).
4) M. Deumie et al., C.R.Hebd.Seances Acad. Sci., Ser.C, 283, 57(1976).
5) T. Nagai et al., Bull.Chem. Soc. Jpn., 47, 1022(1974).

Table IX

Dipole moments of heteroaromatic molecules

V.W.Van der Meer and G.Vertogen proposed that acentral transverse dipoles are important for the tilt alignment in the smectic C phase, based on their dipole-induced dipole model.[26] This theory applies the dipole-induced dipole inter-

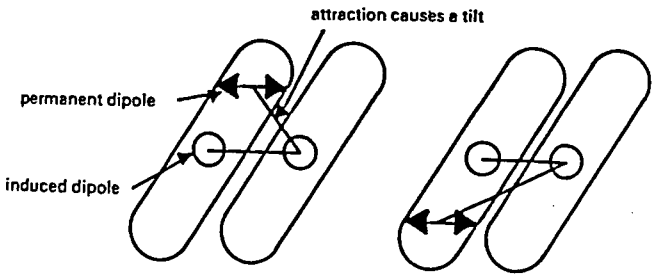

action giving rise to attractive forces among molecules, to the mechanism of tilting within a layer.

From these viewpoints, it could be considered that a large transverse dipole moment of fluorenone causes the smectic C phase in a case of 1d.

Figures 12 and 13 show the mesomorphic trends of the homologous series for 3-(2-hydroxy-4-alkoxybenzylideneamino)-dibenzothiophenes(2b) and 2-(2-hydroxy-4-alkoxybenzylidene-amino)fluorenes(2c), respectively. The transition temperatures of 2b and 2c are listed in Table X and XI, respectively.

The mesomorphic trends of 2b and 2c are normal in the nematic to isotropic and the smectic A to nematic phase transitions, like those of 2a.

The narrower temperature width of the odd-even alternation in the nematic to isotropic phase transition temperatures, rather than that of compounds without a hydroxyl group, is common to 2a, 2b and 2c. This seems to indicate that the molecular interaction among the core moieties in mesophases for 2a, 2b and 2c is stronger than that of non-hydroxyl compounds,

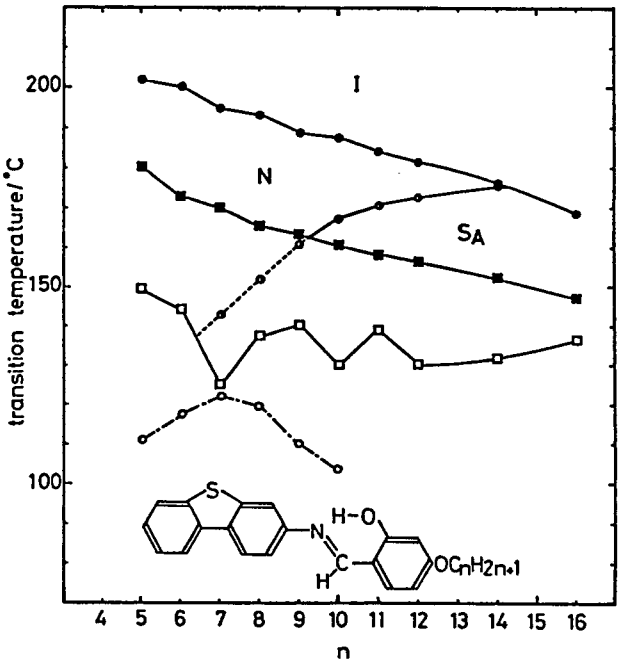

Figure 12 Plots of transition temperatures against the number of carbon atoms(n) in the alkyl chain of 3-(2-hydroxy-4-alkoxybenzylideneamino)dibenzothiophenes(2b). ●;N or S_A-I, ◐;S_A-N, ○;virtual S_C-S_A or N, ■;melting point and □;crystallization on cooling at 5°C/min.

Table X

Phase transition temperatures(T/°C) of 3-(2-hydroxy-4-alkoxybenzylideneamino)dibenzothiophenes(2b)

n	T_{C-S_A} or N	T_{S_A-N} or I	T_{N-I}	$T_{rec.}$	$T_{S_C-S_A}$ or N(virtual)[a]
5	180.1		201.8	149.5	111
6	172.6		200.2	144.0	118
7	170.0	(143.0)[b]	194.6	126.8	122
8	165.5	(151.7)	193.2	137.5	120
9	163.4	(160.7)	188.7	140.3	110
10	160.3	167.0	187.3	129.8	104
11	157.8	170.4	183.9	139.0	
12	156.7	173.7	181.6	130.5	
14	152.4	175.2	176.2	131.5	
16	147.2	168.6		136.6	

a) C:crystal, S_C:smectic C, S_A:smectic A, N:nematic, I:isotropic and rec.:recrystallization (cooling rate:5°C/min.).

b) ( ):monotropic transition.

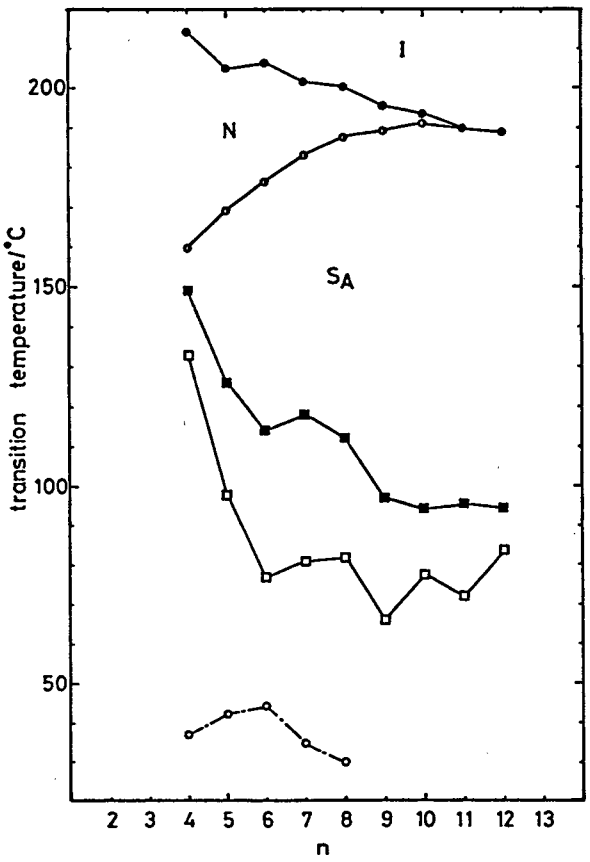

Figure 13

Plots of transition temperatures against the number of carbon atoms(n) in the alkyl chain of 2-(2-hydroxy-4-alkoxybenzylidene-amino)fluorenes(2c).

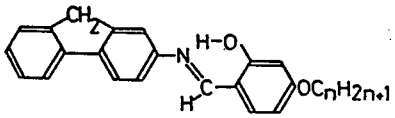

●;S_A or N-I, ◐;S_A-N, ○;virtual S_C-S_A, ■; melting point and □; crystallization on cooling at 5°C/min.

Table XI

Phase transition temepratures(T/°C) of 2-(2-hydroxy-4-alkoxybenzylideneamino)fluorenes(2c)

n	T_{C-S_A} or N	T_{S_A-N} or I	T_{N-I}	$T_{rec.}$	$T_{S_C-S_A}$(virtual)[a]
4	149.3	159.6	214.5	133.0	37
5	126.3	169.1	205.0	97.9	42
6	114.0	176.4	206.6	77.0	44
7	118.3	183.2	201.7	80.8	34.5
8	112.2	187.6	200.5	81.8	29.5
9	97.0	189.0	195.6	66.2	
10	94.4	190.8	193.6	77.5	
11	95.4	189.9		72.1	
12	94.5	188.9		83.7	

a) C:crystal, S_C:smectic C, S_A:smectic A, N:nematic, I:isotropic and rec.:recrystallization (cooling rate:5°C/min.).

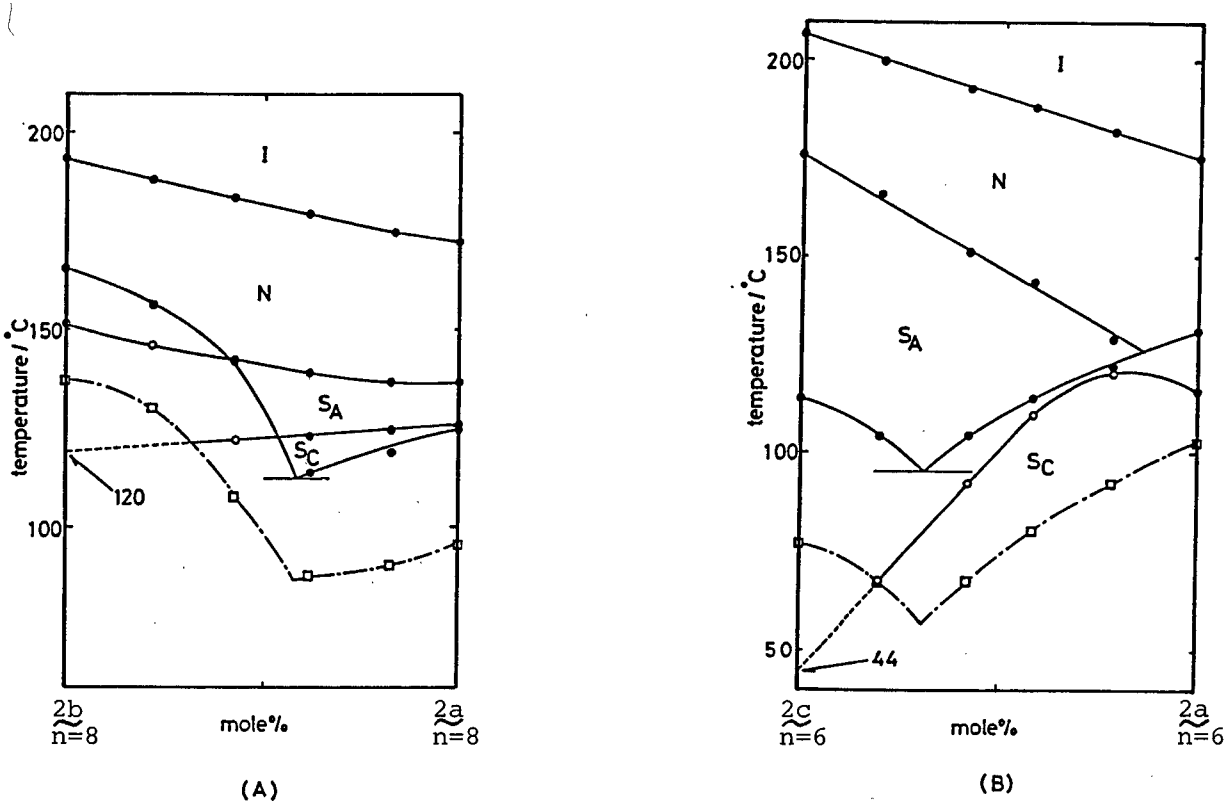

Figure 14 Typical binary phase diagrams for the estimation of the virtual S_C-S_A or N transition temperatures. (A) for 2a(n=8) and 2b(n=8), and (B) for 2a(n=6) and 2c(n=6). □;crystallization temperature on cooling at 5°C/min.

thus leading to decreasing the effect of motions of the terminal alkyl chain on the nematic to isotropic transition temperatures.

The compounds 2b and 2c show no smectic C phase, similar to the corresponding non-hydroxyl compounds 1b and 1c, and the virtual smectic C to smectic A and to nematic phase transition temperatures were estimated by extrapolating the line of smectic C to smectic A or to nematic phase transition temperatures in the binary phase diagram with 2a possessing the same alkyl chain length as that of the compound to be estimated. Typical diagrams are illustrated in Figure 14.

With 2c, the virtual smectic C to smectic A transition temperatures are extremely low, while those of 2b are slightly lower than those of 2a. This situation was made to be clearer in Figure 15, in which the $T_{S_C-S_A}$ or N/T_{N-I} of 2a, 2b and 2c are plotted against the carbon number(n) in the alkyl chain.

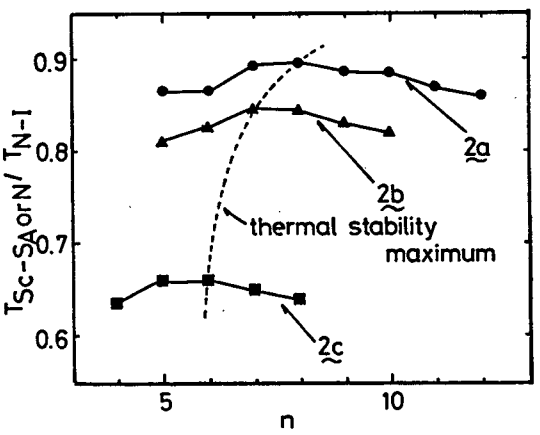

Figure 15 Plots of $T_{S_C-S_A}$ or N/T_{N-I} against the carbon number(n) in the alkyl chain for 2a, 2b and 2c.

Among these three compounds, the difference in the geometrical structure is little as shown in I-1, but the dipole moments differ from each other.

Obviously, the order of the magnitude of the dipole moments of dibenzofuran, dibenzothiophene and fluorene shows a relation to the smectic C thermal stability. In other

words, the smectic C thermal stability of 2a, 2b and 2c increases as the magnitude of a dipole moment of dibenzofuran, dibenzothiophene and fluorene becomes larger.

This fact indicates that the thermal stability of the smectic C phase could be increased by an appropriate magnitude of the transverse dipole moment, even in such an unsymmetrical molecule. In other words, favorable factors for the occurrence of the smectic C phase, being suggested so far, are not always required if the molecule has an appropriate magnitude of the transverse dipole moment. This might indicate that the complemental relation of the transverse dipole moment to the favorable factors exists.

In a case of 1d and 2d, acentral transverse dipole moment in the core moiety seems to be important for the occurrence of the smectic C phase, as V.W.Van der Meer et al. referred to, in a comparison with a case of 1a and 2a. However, in the latter case a hydroxyl group at ortho-site of benzylideneamino moiety, to be considered to locate nearly in the central part of the core, was important for the occurrence of the smectic C phase.

Figure 16 shows a binary phase diagram of 2a(n=8) and DBFOC8OMe, in which a hydroxyl group of 2a was methoxylated, indicating that a methoxy group decreases the mesomorphic thermal stability due to the bulkiness, to result in exhibiting no mesophase. The bulkiness of a methoxy group reduces the T_{S_C-N} more largely as shown by the ratio of T_{S_C-N} of DBFOC8OMe to that of 2a(n=8) calculated to be 0.690, while the ratio of T_{N-I} is 0.730, where the unit of T_{S_C-N} and T_{N-I} is "K". Furthermore, it is more likely that DBFOC8OMe has a formative ability of the smectic C structure rather than that of the smectic A one and

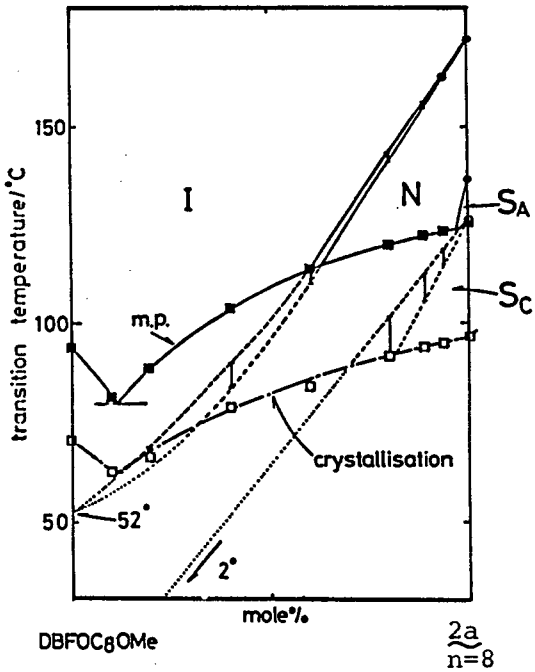

Figure 16 A binary phase diagram of DBFOC8OMe and 2a(n=8).

the estimated T_{S_C-N}/T_{N-I} is 0.846, meaning that the smectic C thermal stability of DBFOC8OMe is lower than that of 2e. However, the thermal stability of the smectic Cphase could be inferred to be larger than that of the smectic A phase for DBFOC8OMe, since the smectic A phase gets in the underlying smectic C phase as seen in Figure 16. Though the bulkiness in the lateral direction is not favored for the occurrence of the smectic C phase as described about 2e, the inference that the smectic C thermal stability is larger than that of the smectic A phase in DBFOC8OMe makes us thought of the importance of the transverse dipole moment even in this case. Thus, it might be indicated that when the molecule has bulky substituents in the lateral direction, leading to the difficulty for forming the smectic A structure, but has

an appropriate magnitude of transverse dipole moments, the smectic C phase take precedence over the smectic A phase.

Though there remains the possibility that the dipole moments of dibenzofuran, dibenzothiophene and fluorene work as "outboard" dipoles, the magnitude of "central" dipoles is also an important factor, since 1a, the non-hydroxyl compounds of 2a, are considered to have extremely low smectic C thermal stability. This means the magnitude of the dipole moment of azomethine linkage is insufficient for the formation of the smectic C phase at such a high temperature. Considering that compounds 1d are smectic C mesogens, these results indicate again that an appropriate magnitude of the transverse dipole moment is required in the core moiety for the formation of the smectic C phase, though the relation of the location of the dipolar part to the smectic C thermal stability is not evident.

As seen in Figures 12 and 13, the positions of the maxima of smectic C thermal stability for 2b and 2c are located at n=7 and n=6, respectively, and the trend of the curves is also "parabolic".

The "parabolic" shapes of smectic C to smectic A and nematic phase transition temepratures for 2a, 2b and 2c are intermediate between those of 5a and 5b, which are steeper and more gently falling, respectively,[22] in the higher homologues. Considering the behaviors of the smectic C thermal stability against the terminal alkyl chain length, it might be indicated that compounds with only one alkyl chain and whose major dipolar parts are more distant from the terminal alkyl group, are more sensitive to the effect of the alkyl chain length as the same case as compounds with small magnitude of the transverse dipole

moment, leading to the importance of dipole-induced dipole interaction for smectic C thermal stability.

The "outboard" dipole moments, in fact, also are thought to be important for the occurrence of the smectic C phase and thus, the transverse dipole moment in the heteroaromatic moiety is considered to work as an "outboard" one in the same manner, as a possibility.

Figure 17 shows the mesomorphic trend of 3d, which an alkyl chain is substituted instead of alkoxy one in 1d.

The layered structural phase, the smectic A phase, is exhibited in the longer alkyl chain than n=14, but a smectic C phase does not appear up to n=14.

A binary phase diagram of 3d(n=12) and 1d(n=11) indicates that the ability to form the smectic C structure is not expected for 3d, as shown in Figure 18, since a succession of the smectic C phase between 3d(n=12) and 1d(n=11) in the phase diagram could not be seen. This system shows a reentrant phenomenon described later.

Therefore, a dipole moment derived from the alkoxy group is crucial for the occurrence of the smectic C phase. Eventually, it seems to be concluded that the transverse dipole moment of a heteroaromatic moiety and the alkoxy dipole moment are in a complemental relation. Thus, the heteroaromatic dipole moment could be interpreted to be an "outboard" dipole moment in a broad sense.

As to the mesomorphic trend of 3d, a characteristic is seen that the nematic to isotropic phase transition temperatures, the mesomorphic thermal stability, keep the level against the change of the terminal alkyl chain length.

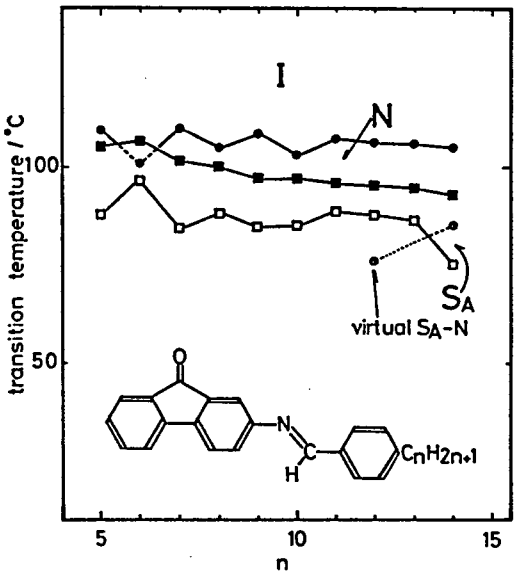

Figure 17 Plots of transition temperatures against the number of carbon atoms(n) in the alkyl chain of 2-(4-alkylbenzylideneamino)-fluorenones(3d). ●;N-I, ◐;S_A-N, ■;melting point and □;crystallization on cooling at 5°C/min.

Table XII

Phase transition temperatures(T/°C) of 2-(4-alkylbenzylideneamino)fluorenones(3d)

n	$T_{C-S_A,N \text{ or } I}$	T_{S_A-N}	T_{N-I}	$T_{cryst.}$ [a]
5	105.2		109.2	88.0
6	106.5		[100.9] [b]	96.7
7	101.6		109.6	84.7
8	100.0		104.8	88.3
9	97.4		108.7	85.2
10	97.0		103.1	85.6
11	96.2		107.4	89.1
12	95.4		106.3	88.0
13	94.7		106.2	86.7
14	92.8	[85.5]	105.2	75.4

a) C:crystal, S_A:smectic A, N:nematic, I:isotropic and cryst:crystallization on cooling at 5°C/min.

b) [ ]:monotropic transition.

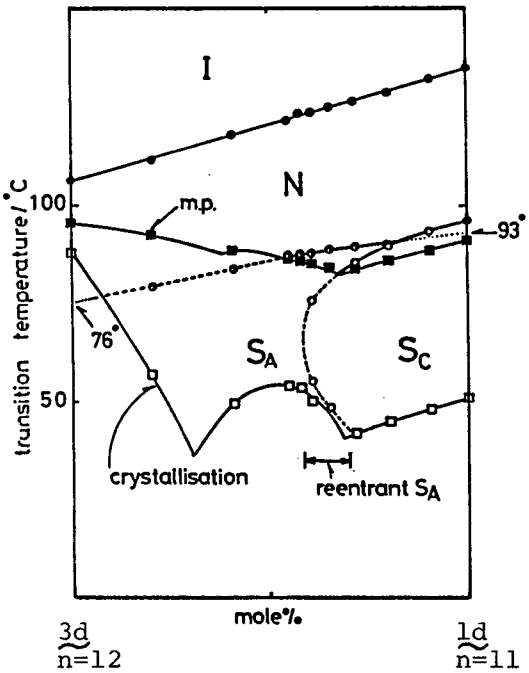

Figure 18 A binary phase diagram of 3d(n=12) and 1d(n=11).

The phase transition temperatures of 2-(4-alkylbenzylideneamino)fluorenones(3d) are listed in Table XII.

Conclusion

3-(2-Hydroxy-4-alkoxybenzylideneamino)dibenzofurans, 3-(2-hydroxy-4-alkoxybenzylideneamino)dibenzothiophenes, 2-(2-hydroxy-4-alkoxybenzylideneamino)fluorenes and 2-(2-hydroxy-4-alkoxybenzylideneamino)fluorenones were prepared and investigated on the mesomorphic behaviors, especially on the occurrence of the smectic C phase.

Through a comparison with 2-(4-alkoxybenzylideneamino)-fluorenones, which have already reported and were reexamined

in this work, the transverse dipole moment was concluded to be an important factor for the occurrence of the smectic C phase. Furthermore, a complemental relation of the transverse dipole moment to the favorable factors for the occurrence of the smectic C phase being suggested so far, are indicated. Consequently, it was shown that the smectic C thermal stability could be raised as the magnitude of the transverse dipole moment increases.

I — 3 New binary systems exhibiting a N-S_A-S_C-S_A reentrant phenomenon

Since the reentrant nematic phase was discovered for a binary mixture of terminal polar mesogens by P.E.Cladis in 1975,[27] the reentrant phenomena of mesophases have been actively studied.

Generally, mesogens exhibiting reentrant phenomena have a strongly dipolar substituent, such as cyano or nitro groups at the terminal part in the core moiety[28] but in some cases a binary mixture of terminal non-polar mesogens also exhibits a reentrant phenomenon.[29]

Recently, a new polymorphism variant N-S_A-S_C-S_A has been reported for the binary mixture of terminal non-polar compounds 6a and 6b, which are structurally similar to each other, although one has two alkyl chains and the other has only one

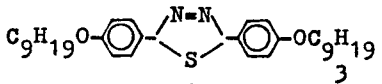

K 97 S_C 192 Is

6a

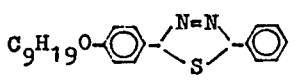

K 96 S_A 126 Is

6b

alkyl chain.[30]

As described before, 2-(4-tridecyloxybenzylideneamino)-fluorenone(1d;n=13) does not show the smectic C phase, while the dodecyloxy derivative(1d;n=12) is a smectic C mesogen. The smectic C phase suddenly disappears at n=13, whilst the smectic C thermal stability increases as the chain length elongates up to n=12.

In order to estimate the virtual smectic C to smectic A

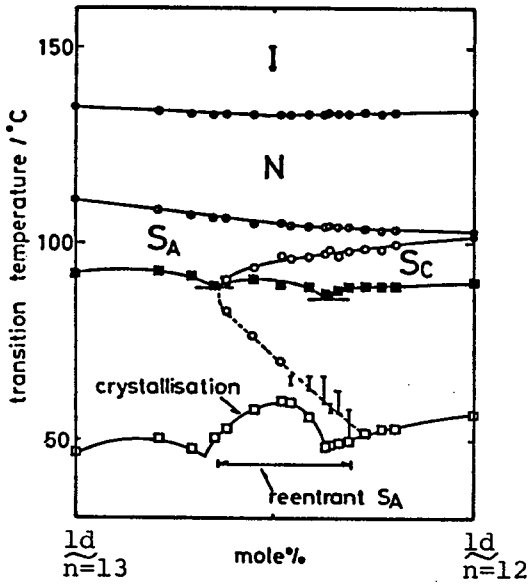

Figure 19 A binary phase diagram of 1d(n=13) and 1d(n=12).

transition temperature of 1d(n=13), a binary phase diagram of these two mesogens was investigated, as shown in Figure 19.

This diagram shows the existence of a reentrant smectic A phase in a range between 36 and 71 mole% of 1d(n=12). The range where the reentrant smectic A phase appears is larger than that of the mixture of 6a and 6b(2 mole%).

The conoscopic observation ascertained the lower smectic phase underlying the smectic C phase to be uniaxial, as seen in Figure 20. A texture of the smectic C phase appearing in the homeotropic area of the smectic A phase is shown in Figure 21.

According to the results of X-ray diffraction, the layer spacings of the smectic A, smectic C and reentrant smectic A phases were found to be 33.38, 32.81 and 32.86A, respectively, for the mixture of 50 mole% of 1d(n=12). The molecular length

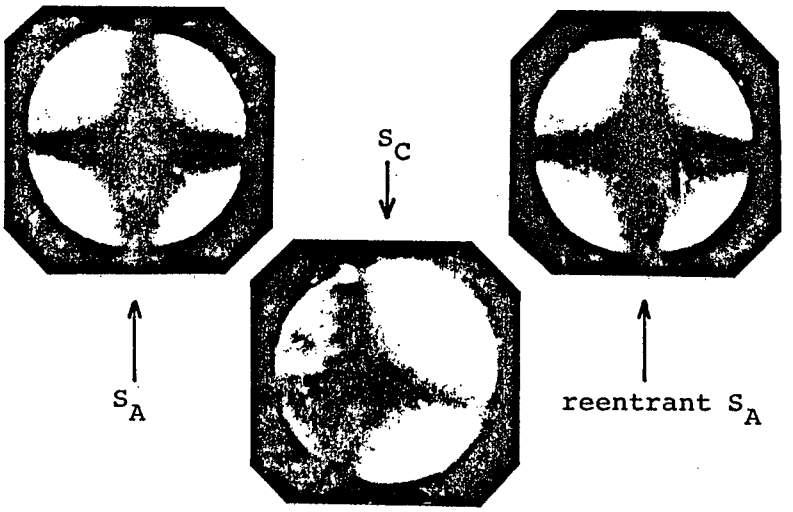

Figure 20 Conoscopic interference figure of S_A (100°C), S_C(90°C) and reentrant S_A(65°C) phases for the mixture of 49 mole% of 1d(n=12).

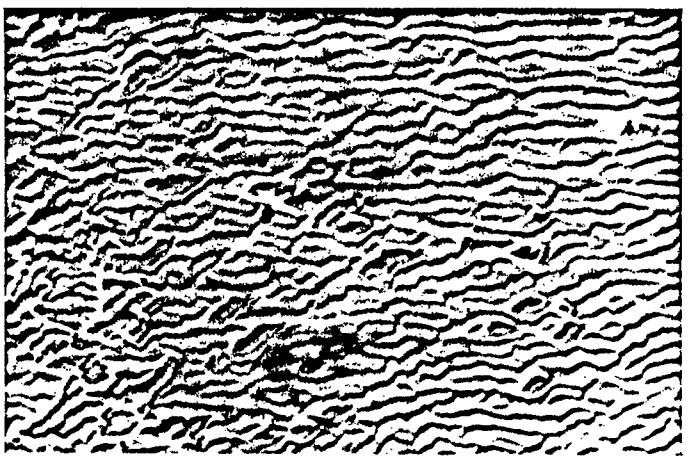

Figure 21 A texture of the smectic C phase at 90 °C for the mixture of 49 mole% of 1d(n=12). This texture appears in the homeotropic area in the smectic A phase on cooling.

with an extended chain is estimated to be 31.5 and 32.7A for the dodecyloxy and tridecyloxy derivatives, respectively. The resulting values of the layer spacings mean that all the smectic phases have a monolayered structure. This indicates that the change of the layer structure, mono- and bi-layers, could not contribute to the origin of this case.

A tilt angle in the smectic C phase for the mixture of 50 mole% of 1d(n=12) is calculated to be about 10° and appeared to be of temperature-independent.

This type of the reentrant phenomenon, a $N\text{-}S_A\text{-}S_C\text{-}S_A$ type, was also seen in a binary system of 1d(n=11) and 3d(n=12), as already shown in Figure 18.

Furthermore, Figure 22 shows the range exhibiting the reentrant smectic A phase becomes narrower as one component showing no smectic C phase is changed to that with a longer alkyl chain.

In Figure 19 and 22, the line of $T_{reS_A\text{-}S_C}$ seems to approach to one point, that is the temperature about 35°C as the concentration of 1d(n=12) becomes close to 100%. This might indicate that the fluorenone liquid crystals 1d are intrinsically reentrant smectic A mesogens.

Conclusion

New binary systems exhibiting a $N\text{-}S_A\text{-}S_C\text{-}S_A$ reentrant phenomenon were found and fluorenone liquid crystals 1d are indicated to have an intrinsic reentrant smectic A mesogenuity as a possibility.

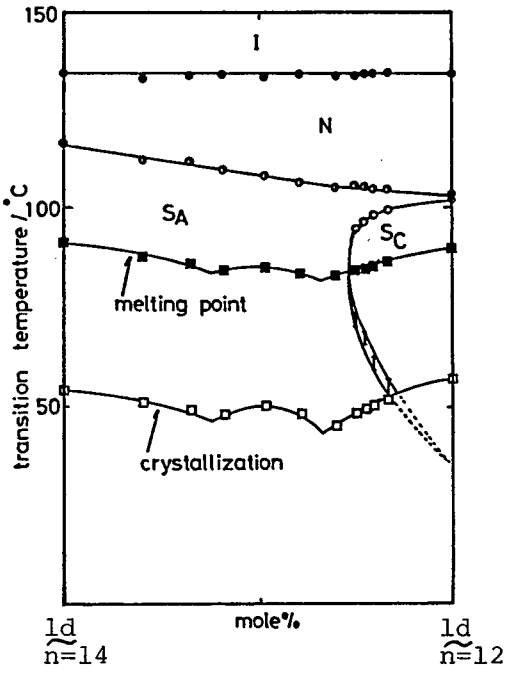

(A)

Figure 22

(A) A binary phase diagram of ld(n=14) and ld(n=12).

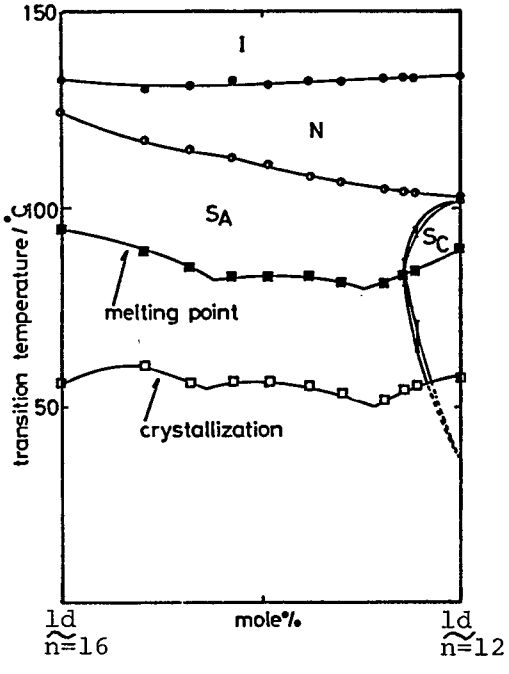

(B)

(B) A binary phase diagram of ld(n=16) and ld(n=12).

EXPERIMENTAL

Preparation of materials

Schiff's base compounds: The Schiff's base compounds were prepared by refluxing the absolute ethanol solution of the equimolar amine and aldehyde and recrystallized from absolute ethanol or hexane more than three times.

All compounds were identified by elemental analylsis, which are given in Table XIII, IR and ^{1}H-NMR spectra.

The following data for the octyloxy compound are typical of the homologous series as a whole:

For 2a(n=8), m/z 415(M^+); $\nu_{max.}$(KBr)3450,3060,2930,2860, 1620,1600,1570,1405,1290,1230,1120,835,820,740 and 720cm^{-1}; δ_H ($CDCl_3$)0.89(3H,t,CH_3), 1.1-2.0(12H,br m,CH_2CH_2), 3.98(2H,t, $ArOCH_2R$), 6.47(1H,d,Ar(5)H), 6.49(1H,s,Ar(3)H), 7.1-7.7(6H,m), 7.90(2H,d,dibenzofuran(1 and 9)H), 8.57(1H,s,CH=N) and 13.62(1H,s,OH).

For 2b(n=8), m/z 431(M^+); $\nu_{max.}$(KBr)3450,3050,2920,2850, 1620,1585,1565,1400,1290,1230,1185,810 and 730cm^{-1}; δ_H($CDCl_3$) 0.89(3H,t,CH_3), 1.1-2.0(12H,br m,CH_2CH_2), 3.98(2H,t,$ArOCH_2R$), 6.47(1H,d,Ar(5)H), 6.50(1H,s,Ar(3)H), 7.1-7.6(4H,m), 7.69(1H, s,dibenzothiophene(3)H), 7.76-7.94(1H,m), 8.57(1H,s,CH=N) and 13.63(1H,s,OH).

For 2c(n=8), m/z 413(M^+); $\nu_{max.}$(KBr)3450,3055,2935,2860, 1630,1600,1570,1455,1405,1305,1235,1175,1145,735 and 725cm^{-1}; δ_H($CDCl_3$)0.89(3H,t,CH_3), 1.1-2.0(12H,br m,CH_2CH_2), 3.91(2H,s, fluorene-CH_2), 3.98(2H,t,$ArOCH_2R$), 6.48(1H,d,Ar(5)H), 6.51(1H, s,Ar(3)H), 7.1-7.6(6H,m), 7.76(2H,d,fluorene(4 and 5)H), 8.56 (1H,s,CH=N) and 13.86(1H,s,OH).

For 2d(n=8), m/z 427(M^+); $\nu_{max.}$(KBr)3370,2920,2850,1715, 1625,1595,1565,1510,1450,1400,1320,1290,1245,1195,1170,1135, 1115,1040,970,875,830,790,765 and 730cm^{-1}; δ_H($CDCl_3$)0.89(3H,t, CH_3), 1.1-2.0(12H,br m,CH_2CH_2), 3.99(2H,t,OCH_2R), 6.4-6.65(2H,m,Ar(5)H and Ar(3)H), 7.1-7.8(8H,m), 8.55(1H,s,CH=N) and 13.34(1H,br s,OH).

For 3d(n=8), m/z 395(M^+); $\nu_{max.}$(KBr)3060,2925,2860,1720, 1610,1600,1575,1510,1450,1310,1250,1200,1175,1040,980,840, 830,770,740 and 730cm^{-1}; δ_H($CDCl_3$)0.89(3H,t,CH_3), 1.1-2.0(12H, br m,CH_2CH_2), 2.69(2H,t,$ArCH_2R$), 7.1-7.7(9H,m), 7.80(2H,d, fluorenone(4) and(5)H) and 8.47(1H,s,CH=N).

Table XIII

Results of elemental analyses

(A) 3-(4-alkoxybenzylideneamino)dibenzofurans(1a)

n	Calcd. /% C	H	N	Found /% C	H	N
1	79.76	5.02	4.65	79.90	4.83	4.60
2	79.98	5.43	4.44	80.21	5.26	4.43
3	80.22	5.81	4.25	80.46	5.72	4.34
4	80.44	6.16	4.08	80.48	6.02	4.13
5	80.64	6.49	3.92	80.65	6.40	3.95
6	80.83	6.78	3.77	80.65	6.67	3.96
7	81.01	7.06	3.63	80.85	6.96	3.80
8	81.17	7.32	3.51	81.26	7.24	3.65
9	81.32	7.56	3.39	81.21	7.71	3.31
10	81.46	7.78	3.28	81.39	7.87	3.20
11	81.59	7.99	3.17	81.45	8.12	3.15
12	81.72	8.18	3.07	81.72	8.31	3.04
14	81.95	8.54	2.90	81.87	8.60	2.86

(B) 3-(4-alkoxybenzylideneamino)dibenzothiophenes (1b)

n	Calcd. /%				Found /%			
	C	H	N	S	C	H	N	S
5	77.18	6.21	3.75	8.58	77.18	6.22	3.61	8.62
6	77.48	6.50	3.61	8.27	77.65	6.47	3.53	8.21
7	77.77	6.78	3.49	7.98	77.60	6.80	3.40	8.00
8	78.03	7.03	3.37	7.71	77.83	7.03	3.29	7.67
9	78.28	7.27	3.26	7.46	78.16	7.23	3.11	7.46
10	78.51	7.50	3.16	7.23	78.36	7.46	3.03	7.24

(C) 2-(4-alkoxybenzylideneamino)fluorenones (1d)

n	Found(%)			Molecular formula	Required(%)		
	C	H	N		C	H	N
6	81.5	6.5	3.5	$C_{26}H_{25}NO_2$	81.4	6.6	3.65
7	81.3	6.7	3.4	$C_{27}H_{27}NO_2$	81.6	6.85	3.5
8	81.6	7.0	3.3	$C_{28}H_{29}NO_2$	81.7	7.1	3.4
9	81.8	7.3	3.2	$C_{29}H_{31}NO_2$	81.85	7.3	3.3
10	81.7	7.5	3.1	$C_{30}H_{33}NO_2$	82.0	7.6	3.2
11	81.9	7.7	3.0	$C_{31}H_{35}NO_2$	82.1	7.8	3.1
12	82.2	8.0	2.9	$C_{32}H_{37}NO_2$	82.2	8.0	3.0
13	82.1	8.2	2.85	$C_{33}H_{39}NO_2$	82.3	8.2	2.9
14	82.15	8.4	2.8	$C_{34}H_{41}NO_2$	82.4	8.3	2.8
16	82.5	8.7	2.6	$C_{36}H_{45}NO_2$	82.6	8.7	2.7
18	82.5	9.0	2.5	$C_{38}H_{49}NO_2$	82.7	8.95	2.5

(D) 3-(2-hydroxy-4-alkoxybenzylideneamino)dibenzofurans (2a)

n	Found(%)			Molecular formula	Required(%)		
	C	H	N		C	H	N
4	76.75	5.87	3.84	$C_{23}H_{21}NO_3$	76.86	5.89	3.90
5	77.12	6.22	3.74	$C_{24}H_{23}NO_3$	77.18	6.21	3.77
6	77.54	6.38	3.59	$C_{25}H_{25}NO_3$	77.49	6.50	3.61
7	77.81	6.75	3.55	$C_{26}H_{27}NO_3$	77.78	6.78	3.49
8	77.86	6.99	3.44	$C_{27}H_{29}NO_3$	78.04	7.03	3.37
9	78.18	7.16	3.23	$C_{28}H_{31}NO_3$	78.29	7.27	3.26
10	78.38	7.46	3.08	$C_{29}H_{33}NO_3$	78.52	7.50	3.16
11	78.68	7.68	3.05	$C_{30}H_{35}NO_3$	78.74	7.71	3.06
12	78.79	7.91	2.83	$C_{31}H_{37}NO_3$	78.95	7.91	2.97
14	79.32	8.28	2.77	$C_{33}H_{41}NO_3$	79.32	8.27	2.80

(E) 3-(2-hydroxy-4-alkoxybenzylideneamino)dibenzothiophenes (2b)

n	Found (%)				Molecular formula	Required (%)			
	C	H	N	S		C	H	N	S
5	73.94	5.83	3.50	8.24	$C_{24}H_{23}NO_2S$	74.01	5.95	3.60	8.23
6	74.12	6.30	3.35	7.97	$C_{25}H_{25}NO_2S$	74.41	6.24	3.47	7.94
7	74.87	6.51	3.33	7.70	$C_{26}H_{27}NO_2S$	74.79	6.52	3.35	7.68
8	75.09	6.76	3.27	7.43	$C_{27}H_{29}NO_2S$	75.14	6.77	3.25	7.43
9	75.32	7.02	3.18	7.14	$C_{28}H_{31}NO_2S$	75.47	7.01	3.14	7.19
10	75.61	7.34	2.93	7.09	$C_{29}H_{33}NO_2S$	75.78	7.24	3.05	6.97
11	75.85	7.52	2.83	6.80	$C_{30}H_{35}NO_2S$	76.07	7.45	2.96	6.77
12	76.23	7.78	2.73	6.53	$C_{31}H_{37}NO_2S$	76.35	7.65	2.87	6.57
14	76.59	8.19	2.58	6.20	$C_{33}H_{41}NO_2S$	76.85	8.01	2.72	6.22
16	77.32	8.66	2.40	5.60	$C_{35}H_{45}NO_2S$	77.30	8.34	2.58	5.90

(F) 2-(2-hydroxy-4-alkoxybenzylideneamino)fluorenes (2c)

n	Found (%)			Molecular formula	Required (%)		
	C	H	N		C	H	N
4	80.49	6.46	3.85	$C_{24}H_{23}NO_2$	80.64	6.49	3.92
5	80.87	6.79	3.72	$C_{25}H_{25}NO_2$	80.83	6.78	3.77
6	80.75	6.99	3.63	$C_{26}H_{27}NO_2$	81.01	7.06	3.63
7	80.92	7.30	3.50	$C_{27}H_{29}NO_2$	81.17	7.32	3.51
8	81.00	7.48	3.35	$C_{28}H_{31}NO_2$	81.32	7.56	3.39
9	81.29	7.76	3.23	$C_{29}H_{33}NO_2$	81.46	7.78	3.28
10	81.21	7.96	3.18	$C_{30}H_{35}NO_2$	81.59	7.99	3.17
11	81.61	8.18	3.09	$C_{31}H_{37}NO_2$	81.71	8.18	3.07
12	81.59	8.38	3.03	$C_{32}H_{39}NO_2$	81.84	8.37	2.98

(G) 2-(2-hydroxy-4-alkoxybenzylideneamino)fluorenones (2d)

n	Found (%)			Molecular formula	Required (%)		
	C	H	N		C	H	N
6	78.15	6.3	3.5	$C_{26}H_{25}NO_3$	78.2	6.3	3.5
7	78.4	6.55	3.4	$C_{27}H_{27}NO_3$	78.4	6.6	3.4
8	78.6	6.8	3.2	$C_{28}H_{29}NO_3$	78.7	6.8	3.3
9	78.7	7.0	3.1	$C_{29}H_{31}NO_3$	78.9	7.1	3.2
10	79.0	7.3	3.0	$C_{30}H_{33}NO_3$	79.1	7.3	3.1
11	79.1	7.5	2.9	$C_{31}H_{35}NO_3$	79.3	7.5	3.0
12	79.35	7.65	2.9	$C_{32}H_{37}NO_3$	79.5	7.7	2.9
13	79.3	7.8	2.8	$C_{33}H_{39}NO_3$	79.6	7.9	2.8
14	79.5	8.1	2.6	$C_{34}H_{41}NO_3$	79.8	8.1	2.7
16	80.0	8.4	2.5	$C_{36}H_{45}NO_3$	80.1	8.4	2.6
18	80.2	8.65	2.4	$C_{38}H_{49}NO_3$	80.4	8.7	2.5
22	80.6	9.2	2.2	$C_{42}H_{57}NO_3$	80.85	9.2	2.2

(H) 2-(2-hydroxy-4-alkoxybenzylideneamino)-9-methylcarbazoles (2e)

n	Found%			Required%		
	C	H	N	C	H	N
4	77.32	6.43	7.40	77.39	6.49	7.52
5	77.68	6.72	7.23	77.69	6.78	7.25
6	77.71	7.00	7.07	77.97	7.05	6.99
7	77.95	7.24	7.00	78.23	7.29	6.76
8	78.37	7.48	6.53	78.47	7.53	6.54
9	78.78	7.71	6.42	78.70	7.74	6.33
10	78.67	7.94	6.34	78.91	7.95	6.13
11	78.97	8.13	5.98	79.11	8.14	5.95
12	79.13	8.36	5.64	79.30	8.32	5.78
14	79.50	8.67	5.43	79.65	8.65	5.46

(I) 2-(4-alkylbenzylideneamino) fluorenones (3d)

n	Found%			Required%		
	C	H	N	C	H	N
5	84.69	6.47	4.11	84.95	6.56	3.96
6	84.73	6.81	3.76	84.98	6.86	3.81
7	84.82	7.06	3.69	85.00	7.13	3.67
8	84.73	7.34	3.53	85.02	7.39	3.54
9	84.90	7.61	3.31	85.05	7.63	3.42
10	84.92	7.83	3.26	85.06	7.85	3.31
11	84.89	8.04	3.16	85.08	8.06	3.20
12	84.85	8.25	3.24	85.10	8.26	3.10
13	84.88	8.42	3.21	85.12	8.44	3.01
14	84.98	8.58	2.87	85.13	8.61	2.92

4-Substituted benzaldehydes: 4-Alkyl-[31], and 4-alkoxybenzaldehydes[32] were purified by column chromatography (silica-gel, benzene-hexane) or by distillation. 2-Hydroxy-4-alkoxybenzaldehydes were prepared by refluxing the mixture of the corresponding alkyl bromide and the equimolar 2,4-dihydroxybenzaldehyde in methanol containing KOH and purified by column chromatography (silica-gel, benzene-hexane).

Heteroaromatic amines: 3-Aminodibenzofuran and 2-aminofluorene were prepared by the catalytic hydrogenation(Pd/C in ethanol) of the nitro derivatives, followed by normal nitration of aromatics, and purified by column chromatography(silica-gel, benzene) and recrystallization from benzene-hexane.

3-Aminodibenzothiophene was prepared from 3-nitrodibenzothiophene-5-oxide, synthesized from dibenzothiophene.[33]

2-Aminofluorenone was prepared according to the literature.[34]

2-Amino-9-methylcarbazole was prepared through steps of 9-methylation, 2-nitration and catalytic hydrogenation from carbazole.

Measurements

Measurements of transition temperatures and microscopic observations of textures of mesophases were made using a Nikon polarizing microscope in conjunction with a Mettler FP52 heating stage and FP5 control unit. Transition enthalpies were measured with a Daini Seikosha differential scanning calorimeter, model SSC-560S. ^{1}H-NMR spectra were measured for solutions in $CDCl_3$ with tetramethylsilane as the internal standard with a JNM-PS-100 NMR spectrometer. IR spectra were recorded for KBr discs with a Hitachi 215 grating infrared spectrophotometer. Mass spectra were determined with a Hitachi RMV-6T mass spectrometer. UV-Visible absorption spectra were measured with a Hitachi 220 double beam UV-Visible spectrometer.

The X-ray studies were made with CuKα radiation on the sample in a capillary tube, and the sample alignment was produced by slowly cooling in a magnetic field.

REFERENCES

1) G.W.Gray, J.B.Hartley, A.Ibbotson and B.Jones, J.Chem.Soc., 4359(1955).
2) K.Shigeta, N.Inoue, J.Nakauchi, M.Yokoyama, M.Nojima, H. Mikawa and S.Kusabayashi, in preparation.
3) D.J.Byron, D.J.Harwood and R.C.Wilson, J.Chem.Soc.,Perkin Trans.2, 197(1983);B.A.Behnam and D.M.Hall, J.Chem.Soc., Perkin Trans.2, 465(1982).
4) G.W.Gray, J.Chem.Soc., 552(1958).
5) W.H.de Jeu, J.Van der Veen and W.J.Goossens, Solid State Commun., 12, 405(1973);J.Van der Veen, J.de Phys., 36, C1-375(1975);W.H.de Jeu and J.Van der Veen, Mol.Cryst.Liq. Cryst., 40, 1(1977);R.Alben, Mol.Cryst.Liq.Cryst., 13, 193 (1971).
6) H.B.Bürgi and J.D.Dunitz, Helv.Chim.Acta, 53, 1747(1970).
7) R.Akaba, K.Tokumaru and T.Kobayashi, Bull.Chem.Soc.Jpn., 53, 1993(1980).
8) P.Skrabal, J.Steiger and H.Zollinger, Helv.Chim.Acta, 58, 800(1975).
9) E.A.Braude and F.Sondheimer, J.Chem.Soc., 3754(1955).
10) J.Bernstein, Y.M.Engel and A.T.Hagler, J.Chem.Phys., 75, 2346(1981).
11) A.Banerjee, Acta Cryst., B29, 2070(1973)
12) O.Dideberg, L.Dupont and J.M.André, Acta Cryst., B28, 1002 (1972).
13) R.M.Schaffrin and J.Trotter, J.Chem.Soc.A, 1561(1970).
14) K.J.Miller and J.A.Savchik, J.Am.Chem.Soc., 101, 7206(1979).
15) J.P.Canselier and C.Clément, J.Chim.Phys.,Phys.-Chem.Biol., 76, 699(1979).
16) D.M.Burns and J.Iball, Proc.Roy.Soc., A227, 200(1955).
17) G.M.Brown and M.H.Bortner, Acta Cryst., 7, 139(1954).
18) G.W.Gray and J.W.Goodby, "Smectic Liquid Crystals ——— textures and structures", Leonard Hill, Glasgow and London, 1984.
19) W.L.McMillan, Phys.Rev.A, 8, 1921(1973).
20) A.Wulf, Phys.Rev.A, 11, 365(1975).

21) J.W.Goodby, G.W.Gray and D.G.McDonnell, Mol.Cryst.Liq. Cryst.Lett., 34, 183(1977).
22) G.W.Gray and J.W.Goodby, Mol.Cryst.Liq.Cryst., 37, 157(1976).
23) D.Demus, J.W.Goodby, G.W.Gray and H.Sackmann, Mol.Cryst. Liq.Cryst.Lett., 56, 311(1980).
24) A.Biering, D.Demus, G.W.Gray and H.Sackmann, Mol.Cryst. Liq.Cryst., 28, 275(1974).
25) G.Sigaud, F.Hardouin and M.F.Achard, Solid State Commun., 23, 35(1977).
26) B.W.Van der Meer and G.Vertogen, J.de Phys.Colloq., 40, C3-222(1979).
27) P.E.Cladis, Phys.Rev.Lett., 35, 48(1975).
28) D.Guillon, P.E.Cladis and J.Stamatoff, Phys.Rev.Lett., 41, 1598(1978).
29) S.Diele, G.Pelzl, I.Latif and D.Demus, Mol.Cryst.Liq.Cryst., 92, 27(1983).
30) G.Pelzl, S.Diele, I.Latif, D.Demus, W.Schäfer and H.Zaschke, Mol.Cryst.Liq.Cryst.Lett., 1, 39(1985).
31) A.Reiche, H.Gross and E.Höft, Chem.Ber., 93, 88(1966).
32) G.W.Gray and B.Jones, J.Chem.Soc., 1467(1954).
33) R.K.Brown, R.G.Christiansen and R.B.Sandin, J.Am.Chem.Soc., 70, 1748(1948);W.Tagaki, K.Kikukawa, K.Ando and S.Oae, Chem.Ind., 1624(1964).
34) O.Diels, Chem.Ber., 34, 1758(1901).

CHAPTER II

Phase Transition Behaviors of Disk-like 5,10,15,20-Tetrakis(4-alkylphenyl)porphyrins

Nowadays, many disk-like molecules exhibiting mesophases are found, for example as shown in scheme below, and the molecular structural characteristics are distinguishable. It is seen that the discogens have a rigid central core and four to eight flexible side chains.

Furthermore, discotic mesophases also are classified to several phases dependent on the structure as the mesophases of rod-like molecules are.[1]

On the other hand, it has not been studied whether the discotic phase could have functions as a combination of the molecular ordered assembly with the intrinsic function of the molecules.

From a viewpoint of the functions, porphyrin derivatives

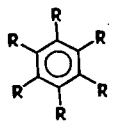

I

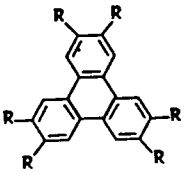

II

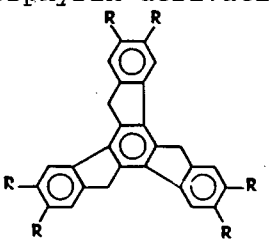

III

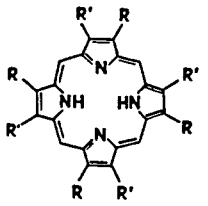

IV

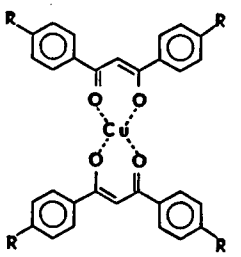

V

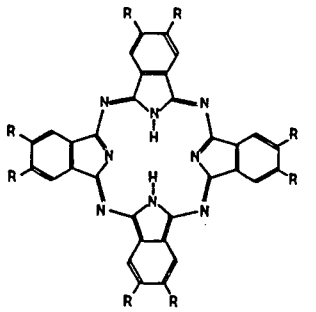

VI

have been extensively studied on available catalysts in organic reactions, model systems in biochemistry,[2] and low-dimentional conductors[3].

Discotic mesogens containing a porphyrin or its analogue have been already reported. i.e. Uro-porphyrin I octa-n-dodecyl-ester(IV)[4], and octa-substituted phthalocyanine(VI) to be a copper complex[5] and a metal-free ligand[6]. However, the former has too narrow mesomorphic thermal range and the latter has too high mesomorphic thermal stability in order to research the functionalized mesophase. Moreover, the synthetic methods of such compounds contain some difficulties. Thus, such porphyrin discotic mesogens with appropriate low thermal stability of mesophases and of which the synthetic route is more simple, are desired.

5,10,15,20-Tetraphenylporphyrin is known to be synthesized by a simple method that is a one-step reaction of pyrrole with benzaldehyde[7], and the process of purification also has been studied[8].

Accordingly, the alkylated and alkoxylated derivatives at 4-site of phenyl group were prepared and investigated on the phase transition behaviors.

5,10,15,20-Tetrakis(4-alkylphenyl)porphyrins(4a) and 5,10,15,20-tetrakis(4-alkoxyphenyl)porphyrins(4b) show considerable differences in the phase transition behaviors to each other.

Figure 1 shows the phase transition trend for the homologous series of 4b. The transition temperatures, enthalpies and entropies are also listed in Table I.

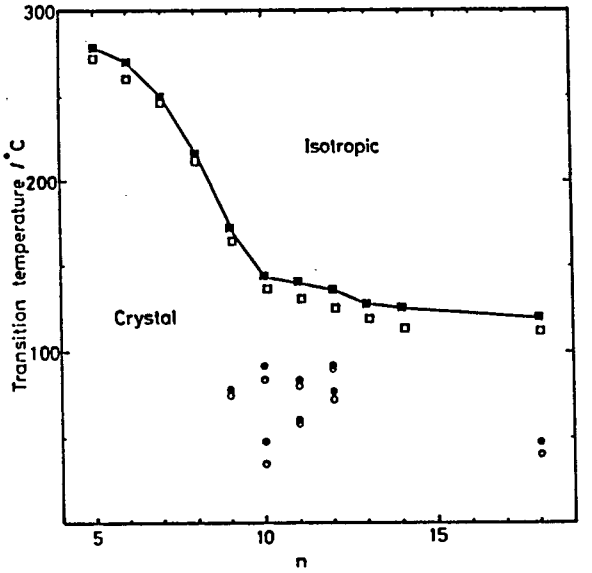

Figure 1 Plots of transition temperatures against the number of carbon atoms(n) in the alkyl chain of 5,10,15,20-tetrakis(4-alkoxyphenyl)porphyrins(4b).

Table I

Phase transition temperatures(T/°C), enthalpies(ΔH/kJ·mol.$^{-1}$) and entropies(ΔS/J·K^{-1}·mol.$^{-1}$) of 5,10,15,20-tetrakis(4-alkoxyphenyl)porphyrins(4b).

n	cryst.—— cryst.			cryst.—— cryst.			cryst.—— iso.		
	T	ΔH	ΔS	T	ΔH	ΔS	T	ΔH	ΔS
5							278.5 [272.0] a)	52.4	95
6							270.5 [259.5]	69.3	128
7							250.0 [246.5]	68.3	130
8							216.5 [212.0]	60.7	124
9				77.5 [75.0]	11.7	33	172.5 [166.0]	59.4	133
10	48.0 [34.5]	7.0	22	91.0 [84.0]	1.5	4.2	144.5 [138.0]	57.7	138
11	58.0 [58.0]	2.0	6.0	83.5 [80.0]	2.0	5.6	140.5 [131.5]	63.4	153
12	77.0 [73.5]	2.9	8.4	92.0 [89.5]	3.5	9.7	136.0 [126.5]	75.2	184
13							128.0 [120.0]	80.8	205
14							125.5 [115.0]	92.6	232
18	47.0 [40.0]	21.1	66				120.5 [112.0]	111.0	282

a) []:transition temperatures on cooling at 5°C/min.

The transition points connected by the line are evidently of the crystal to isotropic liquid transitions. The microscopic observations of the phase underlying the isotropic liquid phase shows the texture is of typical for a crystalline phase. Furthermore, these phase transitions have large enthalpy and entropy changes as shown in Table 1, and in a binary phase diagram of the homologous series(n=11 and n=14), as seen in Figure 2, the eutectic point appeared at 85 mole% of 4b(n=14). These results indicate that the transitions to the isotropic phase are those from the crystalline phase.

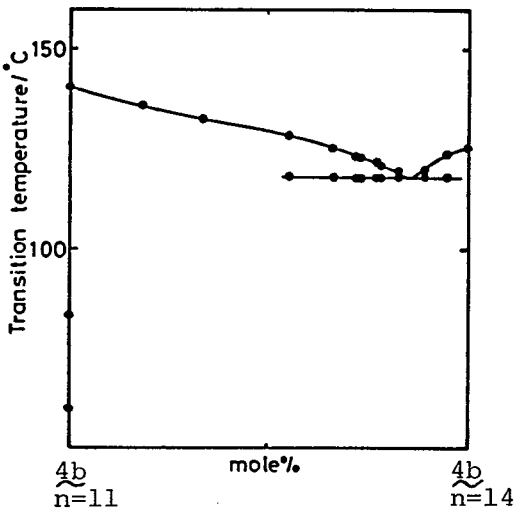

Figure 2 A binary phase diagram of 4b(n=11) and 4b(n=14).

For the other transitions seen in 4b, thus, it is concluded that these transitions are of the solid to soild ones. This is reasonable, considering the transition enthalpy and entropy are far smaller than those of the crystal to isotropic transitions stated above.

On the other hand, alkyl derivatives 4a show the different trend of the phase transitions from those of 4b, which have, moreover, one or two phases between the crystalline and the isotropic phases, as shown in Figure 3. These two phases are named to be m_1 and m_2 phases for the lower and upper phases, respectively.

The enthalpy and entropy changes of the crystal to m_1 phase transition are the largest in all transitions, and the magnitude of them is comparable to that of the crystal to isotropic tran-

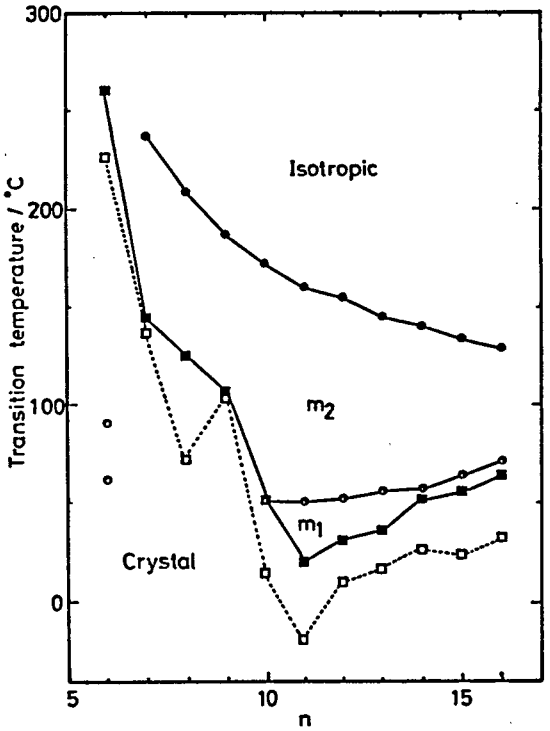

Figure 3 Plots of transition temperatures against the number of carbon atoms(n) in the alkyl chain of 5,10,15,20-tetrakis(4-alkylphenyl)porphyrins(4a).
□;C-m_1 transition on cooling at 5°C/min.

Table II

Phase transition temperatures(T/°C), enthalpies(ΔH/kJ·mol.$^{-1}$) and entropies(ΔS/J·K^{-1}·mol.$^{-1}$) of 5,10,15,20-tetrakis(4-alkylphenyl)porphyrins(4a).

n	Cryst.——m_1 or m_2			m_1——m_2			m_2——Iso.		
	T	ΔH	ΔS	T	ΔH	ΔS	T	ΔH	ΔS
6	84.5 [62.0]	9.0	25				260.0 [226.5]	33.5	63
7	144.5 [137.0]	23.1	55				236.5 [229.5]	28.6	56
8	(71.0	7.5	22)	126.0 [121.5]	23.8	60	208.5 [200.0]	25.0	52
9	107.0 [103.5]	25.4	67				187.0 [183.5]	26.6	58
10	(15.0	8.3	29)	51.5 [46.0]	19.6	61	172.5 [166.0]	25.2	57
11	20.0 [-18.5]	41.7	142	50.5 [50.5]	10.0	31	160.5 [153.0]	23.8	55
12	31.0 [10.5]	46.1	152	52.0 [50.0]	14.0	43	155.0 [149.0]	23.3	54
13	36.0 [17.0]	25.5	82	55.5 [54.5]	16.6	50	145.0 [140.0]	23.9	57
14	52.0 [26.0]	62.6	193	57.0 [55.5]	36.9	112	140.5 [135.0]	24.4	59
15	56.0 [24.0]	92.2	280	65.5 [65.0]	31.4	93	134.5 [130.0]	26.5	65
16	64.5 [33.0]	99.3	289	71.0 [67.5]	34.5	100	129.0 [123.0]	27.2	67

a) [ ]:transition temperatures on cooling at 5°C/min.
b) ( ):These transitions appeared on cooling.

sition ones in 4b. The m_2 to isotropic transition enthalpy and entropy changes are comparable to each other in the homologous series, though there exists a slight change of the magnitude of the enthalpy and entropy with the elongation of terminal alkyl chains. In the m_1 to m_2 phase transition, a variety of the magnitude of the transition enthalpy and entropy changes are seen.

The transition enthalpy and entropy increase as the terminal alkyl chains are elongated. The proportions of the entropy of each transition to the total entropy change are comparable in the homologous series, that is, typically 64, 21 and 15% for the crystal to m_1, m_1 to m_2 and m_2 to isotropic transitions, respectively, in the pentadecyl derivative.

Furthermore, far larger supercooling appears on the crystal-m_1 or m_2 transition than on the other ones. The m_2 to isotropic transition temperatures show a slight odd-even alternation as seen in rod-like liquid crystals.

These results imply that the m_1 and m_2 phases are mesomorphic as a possibility.

Binary phase diagrams of the homologous series indicate that the m_2 phase, at least, is mesomorphic or solid solution, since the continuity of the m_2 phase are seen in Figure 4, where the m_1 phase shows the continuity in a case of the components to be pentadecyl and tridecyl derivatives, though the m_1 phase is discontinuous in a combination of pentadecyl and dodecyl ones.

However, these situations are frequently seen in the mixture of n-parafins. The mixture in such a case are recognized to be solid solution.[9] The states of m_1 and m_2 phases are ap-

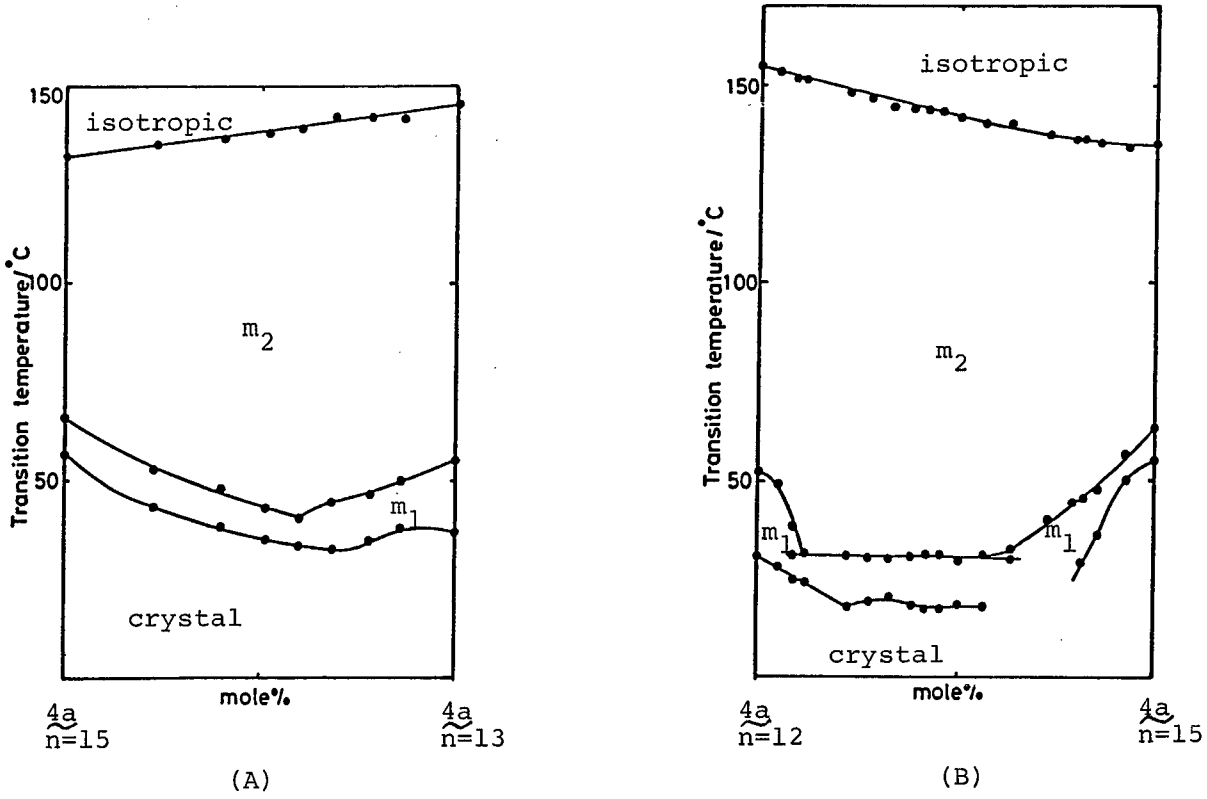

Figure 4 Binary phase diagrams of the homologous series of 4a. (A) for 4a(n=15) and 4a(n=13), and (B) for 4a(n=15) and 4a(n=12).

parently different from that of a brittle crystalline phase. Therefore, the m_1 and m_2 phases may be also considered to be a plastic crystalline phase. According to the proposal by J. Timmermans that the upper limit of the entropy change of fusion is 21 $J \cdot K^{-1} \cdot mol.^{-1}$ for plastic crystalline phase, however, the m_2 to isotropic phase transition entropy is too large to be recognized as a plastic crystalline state.[10]

The changes of the infrared spectra for the phase transitions indicate that the terminal alkyl chains are still in a rigid environment in the m_1 phase, which means the m_1 phase has a three-dimentional structure, since the split of the band at 700-750cm^{-1}, which is assigned to be due to the rocking mode of methylene group in the chains, is kept at the m_1 phase as shown in Figure 5, while in the m_2 phase the band split is broken to be one absorption band as the same as that in the isotropic phase. In this sense, only the m_2 phase has a possibility to be a mesophase. On the other hand, the band split is broken in only the isotropic phase for 4b, meaning the phase underlying the isotropic one has a three-dimentional structure, that is, a crystalline phase to be recognized.[11]

Furthermore, the results of small angle X-ray diffraction study indicate that the m_1 and m_2 phases have a different structure mutually, which are different from that of the crystalline phase, and the diffraction patterns of the m_1 and m_2 phases appear as a crystalline-like one rather than to be mesomorphic.

Therefore, in the m_2 phase the structure is three-dimentional but the alkyl chains are in a liquid-like state. This situation might imply that the m_2 phase is a tegma crystalline one.[12]

Conclusion

It was found that 5,10,15,20-tetrakis(4-alkylphenyl)-porphyrins(4a) have a state in which the core moiety is rigid but the alkyl chains are flexible as in a liquid state.

On the other hand, 5,10,15,20-tetrakis(4-alkoxyphenyl)-porphyrins(4b) show the different behaviors of phase transitions from those of 4a and have simlpy a crystal to isotropic phase transition except for solid-solid ones.

These different behaviors seem to be important to consider the essence of mesomorphic properties of disk-like molecules.

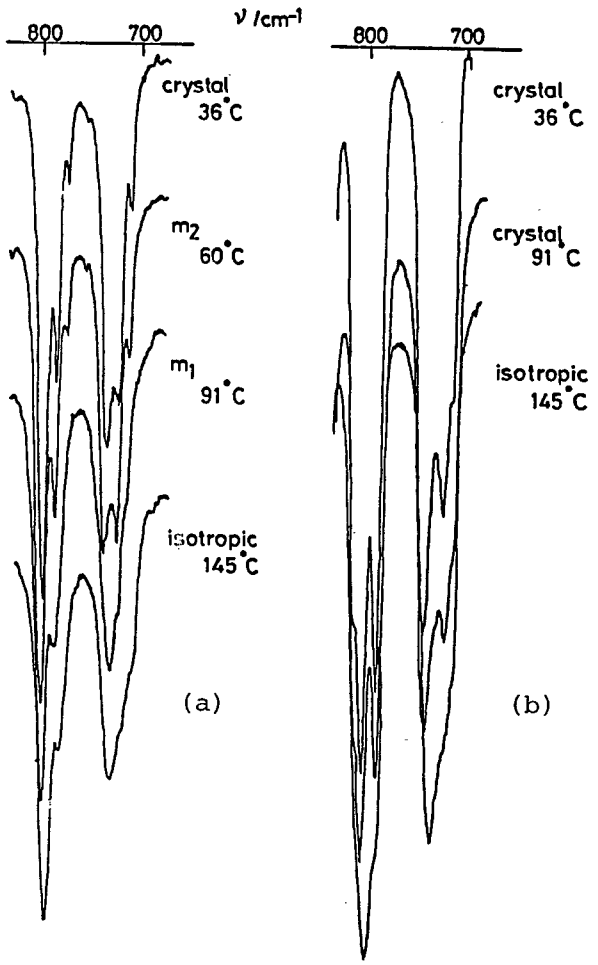

Figure 5 The temperature dependent infrared absorption spectra of (a) 4a:n=15 and (b) 4b:n=14.

EXPERIMENTAL

Preparation of materials

5,10,15,20-Tetrakis(4-alkylphenyl)porphyrins(4a) and 5,10,15,20-tetrakis(4-alkoxyphenyl)porphyrins(4b):Tetraphenylporphyrin derivatives were prepared according to the method of A.D.Adler et al.[7] and the purification followed the methods of G.H.Barnet et al. and K.Roussean et al.[8] in part. The following procedure for a pentadecyl derivative are typical of the homologues of 4a and 4b.

The equimolar 4-pentadecylbenzaldehyde,[13] 5.88g(18.6mmol) and pyrrole, 1.25g(18.6mmol) in 60ml of propionic acid was refluxed for 30min. After cooling the mixture to about 50°C, 60 ml of acetone was added. The mixture was cooled down to room temperature to make porphyrin materials crystallized and the filtration gave crude violet crystals after washing with acetone. This crude material was solved into 50ml of ethanol-free chloroform and 20ml of benzene solution of 0.5g(2.2mmol) of 2,3-dichloro-5,6-dicyanobenzoquinone[DDQ] was added to be refluxed for 3hrs. After the evaporation, the material was purified by column chromatography(400cc of activated alumina with benzene as developing solvent). The material was separated from impurities by Soxhlet extraction with ethanol-methanol(1:1) for 30 hours, and recrystallized from 80ml of benzene-acetone(3:5) to give 0.53g of pentadecyl derivative.

The following data for the pentadecyl and tetradecyloxy derivatives are typical of the other homologues of 4a and 4b, respectively.

For 4a(n=15), $\nu_{max.}$(KBr)3400,3320,3020,2925,2855,1500, 1470,1400,1350,1220,1180,1020,995,980,970,860,845,800,735 and 720cm^{-1};δ_H($CDCl_3$) -2.74(2H,br s,NH), 0.89(12H,t,CH_3), 1.1-2.2 (104H,br m,CH_2CH_2), 2.98(12H,t,$ArCH_2R$), 7.53(8H,d,Ar(3)H), 8.13(8H,d,Ar(2)H) and 8.86(8H,s,pyrrole-H).

For 4b(n=14), $\nu_{max.}$(KBr)3425,3320,3040,2925,2855,1610, 1560,1505,1465,1350,1285,1245,1175,1105,1070,980,970,840,800, 790,740 and 720cm^{-1};δ_H($CDCl_3$) -2.73(2H,br s,NH), 0.89(12H,t, CH_3), 1.1-2.0(96H,br m,CH_2CH_2), 4.18(8H,t,$ArOCH_2R$), 7.22(8H, d,Ar(3)H), 8.08(8H,d,Ar(2)H) and 8.85(8H,s,CH=CH).

Measurements

The textures were observed using a Nikon polarizing microscope in conjunction with a Mettler FP52 heating stage and FP5 control unit. Transition temperatures and enthalpies were measured with a Daini Seikosha diffrential scanning calorimeter, model SSC-560S. Transition entropies were calculated by the relation $\Delta H=T\Delta S$.

^{1}H-NMR spectra were measured for solutions in $CDCl_3$ with tetramethylsilane as the internal standard using a JNM-PS-100 NMR spectrometer. IR spectra were recorded for films with a Hitachi Perkin-Elmer 225 grating infrared spectrophotometer, except for the identification using a Hitachi 215 grating infrared spectrophotometer for KBr disks. UV-Visible absorption spectra were measured with a Hitachi 220 double beam UV-Visible spectrometer.

The small angle X-ray studies were made with CuKα radiation on the sample in a capillary tube, but the sample was not aligned in a magnetic field.

REFERENCES

1) J.C.Dubois and J.Billard, "Liquid Crystals and Ordered Fluids", Vol.4, A.C.Griffin and J.F.Johnson ed., Plenum press, New York, p.1043(1984).

2) "Porphyrins and Metalloporphyrins", K.M.Smith ed., Elsevier, New York, 1975.

3) B.M.Hoffman and J.A.Ibers, Acc.Chem.Res., 16, 15(1983).

4) J.W.Goodby, P.S.Robinson, Boon-keng Teo and P.E.Cladis, Mol.Cryst.Liq.Cryst., 56, 303(1980).

5) C.Piechocki, J.Simon, A.Skoulios, D.Guillon and P.Weber, J.Am.Chem.Soc., 104, 5245(1982).

6) D.Guillon, A.Skoulios, C.Piechocki, J.Simon and P.Weber, Mol.Cryst.Liq.Cryst.,100, 275(1983).

7) A.D.Adler, F.R.Longo, J.D.Finarelli, J.Goldmacher, J.Assour, and L.Korsakoff, J.Org.Chem., 32, 476(1967).

8) G.H.Barnet, M.F.Hudson and K.M.Smith, J.Chem.Soc.Chem.Commun., 1401(1975);K.Rousseau and D.Dolphin, Tetrahedron Lett., 48, 4251(1974).

9) A.R.Ubbelohde, "The Molten State of Matter", John Willey & Sons, Chichester, 1978.

10) J.Timmermans, J.Chim.Phys., 35, 331(1938).

11) R.G.Snyder, J.Mol.Spectrosc., 7, 116(1961).

12) D.Markovitsi, J.Andre, A.Mathis, J.Simon, P.Spegt, G.Weill and M.Ziliox, Chem.Phys.Lett., 104, 46(1984).

13) A.Reiche, H.Gross and E.Höft, Chem.Ber., 93, 88(1966).

CHAPTER III

Photoconducting Behaviors of 2-(2-Hydroxy-4-pentyloxybenzylideneamino)-9-methylcarbazole and 5,10,15,20-Tetrakis(4-pentadecylphenyl)porphyrin

Nematic liquid crystals with rod-like shapes have been limited to be used as switching devices by way of applied electric field. Therefore, the darkcurrent behaviors of the nematic state have been mainly studied so far, while the photocurrent ones have been reported with only a few papers, much less for disk-like liquid crystals.

Studies of photoconducting behaviors in mesophases are interested in (1)searching some new functions of mesophases, (2)researching the molecular interactions in mesophases and (3)revealing the fundamental differences among mesophases, crystalline and isotropic liquid phases in a sense of electric conduction.

Of the photoconduction in mesomorphic states, Kusabayashi and Labes firstly reported for nematic, smectic and cholesteric materials that a photo-response was found in several rod-like liquid crystals.[1] Recently, the photocarrier transport mechanism for the photoconductive 2-(4-decyloxybenzylideneamino)-fluorenone(1d:n=10) in the nematic and smectic states has been suggested that the nature of the photocarrier is not electronic but ionic, and the carrier species are $O_2^{\cdot-}$ and the cation radical derived from the compound itself,[2] generated from the excited state by one photonic process.[3]

On the other hand, Poly(N-vinylcarbazole) have been extensively studied as an available photoconductive polymer and

the carrier generation and transport mechanisms were revealed.[4,5]

The liquid crystalline system containing carbazole as a dopant was also investigated, and the photo-response and photo-conductivity-voltage characteristics were reported.[6]

Any results, however, have not been sufficiently obtained from a viewpoint of differences of photocurrent behaviors among mesophases, crystals and isotropic liquid phase.

In order to compare the behaviors of photoconduction in mesophases with those of crystalline and isotropic phases, 2-(2-hydroxy-4-pentyloxybenzylideneamino)-9-methylcarbazole(2e: n=5) was selected to be investigated on the photoconducting behaviors, as a rod-like mesogen.

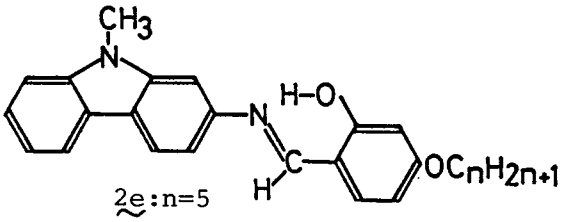

2e:n=5

On the other hand, 5,10,15,20-tetrakis(4-pentadecylphenyl)-porphyrin(4a:n=15) was investigated on the photoconducting behaviors in relation to the phase transitions.

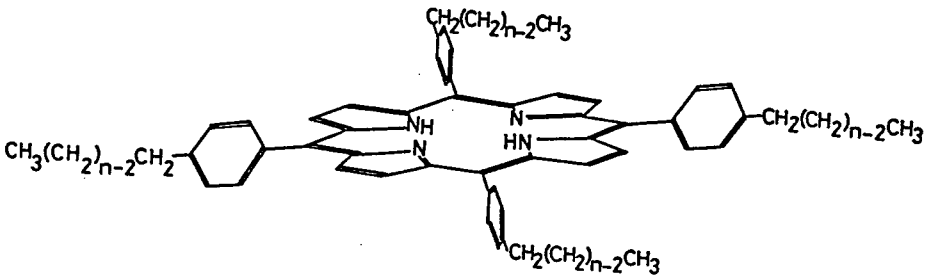

4a:n=15

5,10,15,20-Tetraphenylporphyrin has been extensively studied from photo-electrochemical viewpoints. In many cases, cells used so far were of Schottky type, leading to the extrinsic

carrier generation.[7]

Generally, the porphyrin compounds are far less soluble into many organic solvents. This means occasionally that the difficulty arises as it should be treated in column chromatography etc.

Tetraphenylporphyrins with long aliphatic chains like 4a and 4b, however, have large solubility into general organic solvents, for example, non-polar solvents as benzene and hexane as well as polar ones as diethylether, chroloform and dichrolomethane. This means that 4a and 4b are suitable for using a spin-coating technique. Thus, long aliphatic derivatives of tetraphenylporphyrins, 4a and 4b, are also interesting from a viewpoint of applications.

Furthermore, 4a have several condensed phases as described in chapter II and it seems to be useful for searching the natures of the individual phases to investigate on photoconducting behaviors with phase transitions.

EXPERIMENTAL

Materials

2-(2-Hydroxy-4-pentyloxybenzylideneamino)-9-methylcarbazole(2e:n=5) and 5,10,15,20-tetrakis(4-pentadecylphenyl)porphyrin (4a:n=15) were prepared by the methods as described in chapter I and II, respectively.

Measurements

The experimental methods of measuring the photocurrent and the darkcurrent for 2e(n=5) are in common with those for 4a(n=15).

The sample cells used for measurements were of sandwich type, consisting of two SnO_2 coated quartz glass electrodes and polyimide film as a spacer. The cell thickness was changeable, depending on the film thickness to be 25μm and 50μm. For a 6μm-thick cell of 4a, polycarbonate film was used. The effective electrode area was $1cm^2$.

The empty cell was set on the heating stage in a cryostat and the sample was injected into the cell space by capillarity at the higher temperature than that of the phase transition to the isotropic liquid, but below 150°C. Once the cell was cooled down to room temperature to crystallize the sample and the system was pumped down for about an hour and replaced with dry nitrogen. All measurements were carried out in dry nitrogen atmosphere.

The typical experimental apparatus for measurements is illustrated in Figure 1. A 500W Xenon lamp was used as a light source and the incident light was introduced to a Bausch and Lomb monochrometer grating 1200 grooves through a water filter.

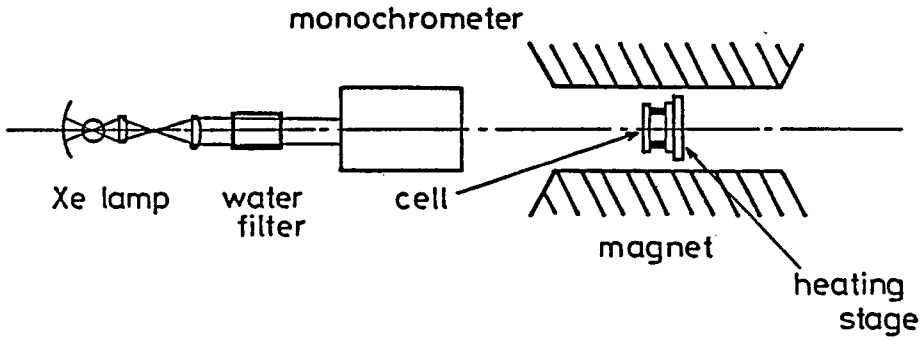

Figure 1 Schematic representation of the experimental apparatus.

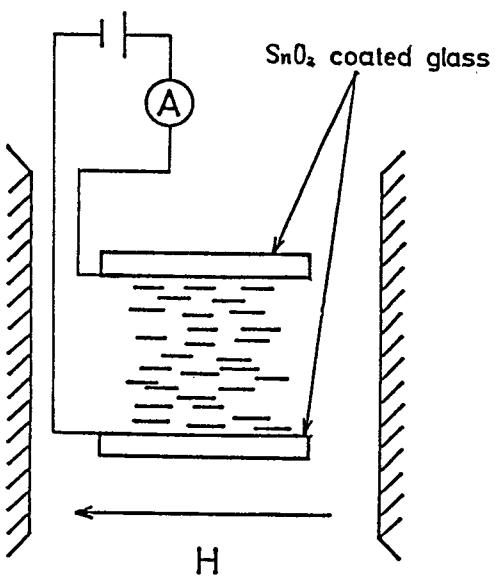

Figure 2 Schematic representation of the cell and the contained rod-like molecules align in a magnetic field to be homogeneous.

The light intensity was measured by Eppley thermopile No22087 of which electromotive force was detected by a microvolt-meter (Tokyo Riko).

A circuit for current-measurements also is illustrated in Figure 2, with a homogeneous alignment of rod-like molecules in a magnetic field. Currents were measured with Takedariken electrometer, TR8651. The electric field was applied by dry batteries, which was detected by Leader Electronics digital multimeter, LDM-853.

For a rod-like liquid crystal 2e, all measurements in the nematic state carried out for the homogeneous alignment cell caused by 5kG of magnetic field. This magnitude of the magnetic field was large enough to fully align the rod-like molecules to be homogeneous in the cell. On the other hand, for a 4a(n=15) no magnetic field was applied for the measurements.

The cryostat used for measurements was with a built-in heating stage, on which the temperature could be controlled by Chino digital-programmed temperature regulator, DP1110 with a thyristor and the temperature was detected by Cu-constantan thermocouple in conjunction with the regulator. The current was recorded by a Hitachi recorder, type 056.

The anisotropy of the dielectric constant of 2e, $\Delta\varepsilon=\varepsilon_{/\!/}-\varepsilon_{\perp}$ where $\varepsilon_{/\!/}$ and $\varepsilon_{\perp}$ are dielectric constants along and perpendicular to the molecular long axis, respectively, were measured for 25μm-thick cell with 0.25cm^2 of the electrode area in 10kG of magnetic field at 1kHz(0.0395V), using a Ando electric TR-10C bridge in connection with a equilibrium point detector, BDA-9 and a frequency transmitter, WBG-9.

III—1 Photoconducting behaviors of a nematogenic 2-(2-hydroxy-4-pentyloxybenzylideneamino)-9-methylcarbazole

The symmetrical cell exhibited the photo-response in the absorbing region of 2e, less than about 550nm. Moreover, in the longer wavelength region where 2e seems not to have apparently absorption, the photo-response was shown, though it was small. Figure 3 shows the absorption and action spectra in the nematic state(120°C) of 2e(n=15). There appeared no differences of the action spectra between the positive and negative electrode illumination except for the magnitude of the photocurrent. The photocurrent for a positive electrode illumination is larger than that for a negative one on the whole.

The action spectrum in the nematic state was found to be

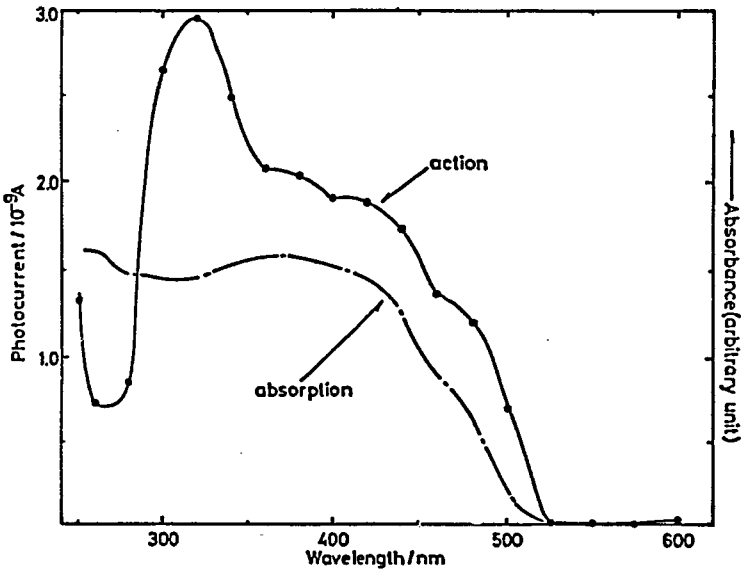

Figure 3 Absorption and action spectra for a film of 2-(2-hydroxy-4-pentyloxybenzylideneamino)-9-methylcarbazole(2e:n=5) in the nematic state(120°C). The action spectrum is that at zero bias.

coincidence with the absorption spectrum of a film in shape, in the longer wavelength region than 360nm. The broken coincidence between the two spectra, however, appeared in the shorter wavelength region. This seems to be due to a light-absorption of the electrode, SnO_2 itself.

On the other hand, the light exponent σ was obtained from plots of photocurrent against the incident light intensity, which appeared to have a good linearity as shown in Figure 4, to be 0.56. This value and the coincidence of the action spectrum with the absorption one mean that the charge carrier generation is caused by way of an extrinsic mechanism in the presence of recombination.[8]

This extrinsic process could be supported by the fact that photoelectromotive force and photocurrent at zero bias are exhibited(see Figure 6,7 and 8). This result also indicates that the SnO_2-$\underset{\sim}{2e}$ interface is photoactive, and considering a fact that the photocurrent increases as oxygen is introduced into the cryostat, the photocurrent of $\underset{\sim}{2e}$ is inferred to be caused by the interaction among SnO_2, O_2 and molecules of $\underset{\sim}{2e}$.

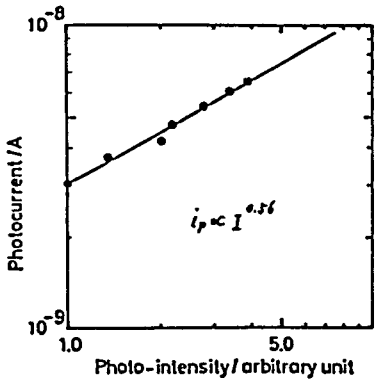

Figure 4 A plot of the photocurrent vs. incident light intensity of 400nm at 20.8V/cm.

Figure 5 shows the temperature dependence of the dark- and photo-current of $\underset{\sim}{2e}$. The normal behavior is seen for the darkcurrent and the conductivities of the crystalline, nematic and isotropic liquid phases are in the order of

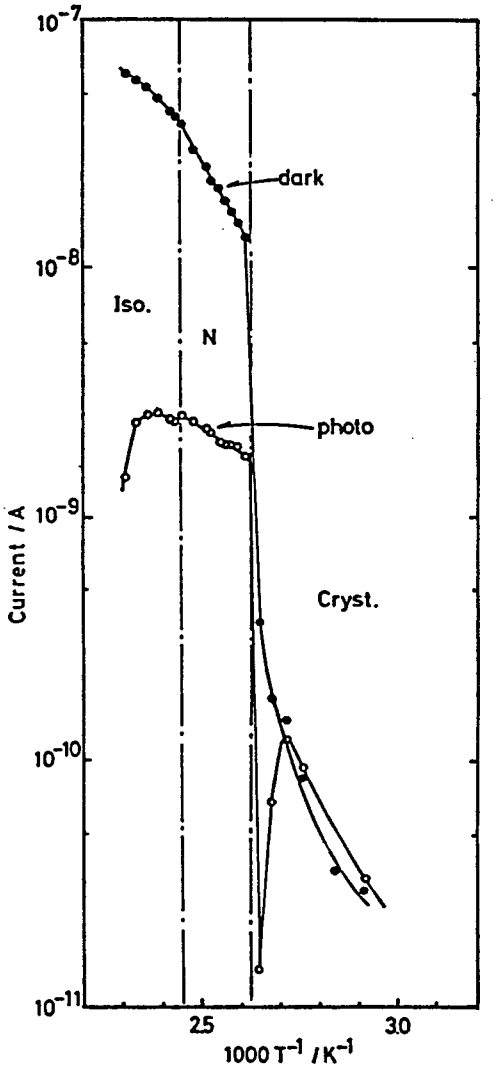

Figure 5 Temperature dependence of the dark- and photo-current for a film of 2-(2-hydroxy-4-pentyloxybenzylideneamino)-9-methylcarbazole(2e:n=5). The photocurrent is for the positive electrode illumination at 20.8V/cm.

less than 10^{-12}, 10^{-10} and 10^{-9} $S \cdot cm^{-1}$, respectively. The activation energies for conduction ΔE were calculated to be 0.36 and 0.56eV for the isotropic and nematic phases, respectively. The darkcurrent is shown to drastically increase at the crystal to nematic phase transition.

On the other hand, the photocurrent also exhibits a large increase at the crystal to nematic transition. However, the magnitude of the photocurrent in the phases with fluidity is smaller than that of the darkcurrent by about one order, while in the crystalline phase, the difference appears to be small. The activation energies for photoconduction ΔE_p^+ were calculated to be 0.17 and 0.19eV for the isotropic and nematic phases, respectively. The difference of the activation energies between the dark- and photo-current implies that the carrier species contributed to the photocurrent are different from those to the darkcurrent. Furthermore, the sudden decrease of the photocurrent is seen near the crystal to nematic transition on heating run, which seems to be caused by the pretransitional phenomena.

The temperature dependence of the photoelectromotive force shows the inverse case against that of the photocurrent, that is, the photoinduced voltage decreases as the temperature is elevated through the crystalline, nematic and isotropic phases and the sign of illuminated electrode appeared to be positive, which is ascertained by the fact that the photocurrent increases in addition to the darkcurrent when the positive electrode is illuminated, but the negative electrode illumination decreases the darkcurrent, in a extreme case as the applied voltage is

too small and the incident light intensity is large, the direction of current is reversed. Therefore, the photocurrent could be considered to be due to the space-charge limited current, as Okamoto et al. referred to.[2]

Figure 6 shows the current-voltage characteristics for the nematic state, where the darkcurrent appeared to be ohmic in the range less than 600Vcm^{-1}. However, the photocurrent exhibits a curious behavior, that in the case of the positive electrode illumination, as the field strength becomes larger, the current increases with non-linearity and once dcreases with a minimum at about 600Vcm^{-1}, and the current again increases. This situation rather resembles to that of tunnel diode, the negative resistance.[9] In the case of the negative electrode illumination, also such a situation appeared, but

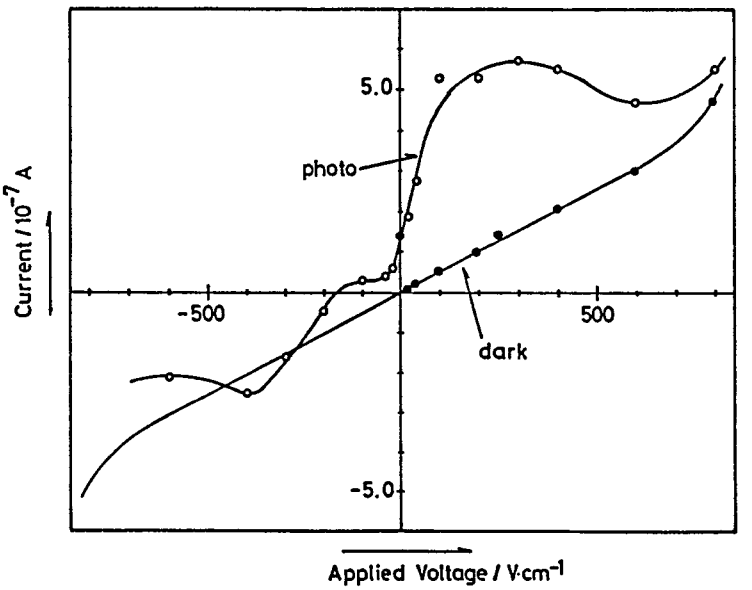

Figure 6 Current-voltage characteristics for a film of 2-(2-hydroxy-4-pentyloxybenzylideneamino)-9-methylcarbazole(2e:n=5) in the nematic state(120°C). The wavelength of the incident light is 400nm.

in the range of 0-200Vcm^{-1}, a rectification behavior was exhibited, implying that the excitons of molecules 2e could interact with the bands of SnO_2 since such a rectification was not found in the darkcurrent behavior.

It has been known, however, that the rod-like liquid crystals of n-type exhibit a dynamic scattering mode beyond the threshold voltage.[10] This 9-methylcarbazole liquid crystal 2e is of negative type, of which the dielectric anisotropy was measured to be -1.0 at 120°C. By microscopic observations, the molecules align homogeneously on the coated SnO_2 film and the Williams domain was formed over 3.84V(1536Vcm^{-1}) of a direct voltage. Thus, the range exhibiting the behavior like a negative resistance for 2e is considered not to be contained in the range in which the Williams domain occurs, meaning that the apparent negative resistance is not due to the molecular random flow.

This consideration was also supported by the current-voltage characteristics for the isotropic liquid phase, as shown in Figure 7. The negative resistance was apparently exhibited even in the isotropic liquid phase, though the maximum and minimum points are different from those in the nematic phase, positionally.

On the other hand, the current-voltage characteristics for the crystalline phase showed a different behavior. The photocurrent little changes as the field strength is elevated up to 40000Vcm^{-1}, while the darkcurrent increases as seen in Figure 8.

These results indicate that though the applied field

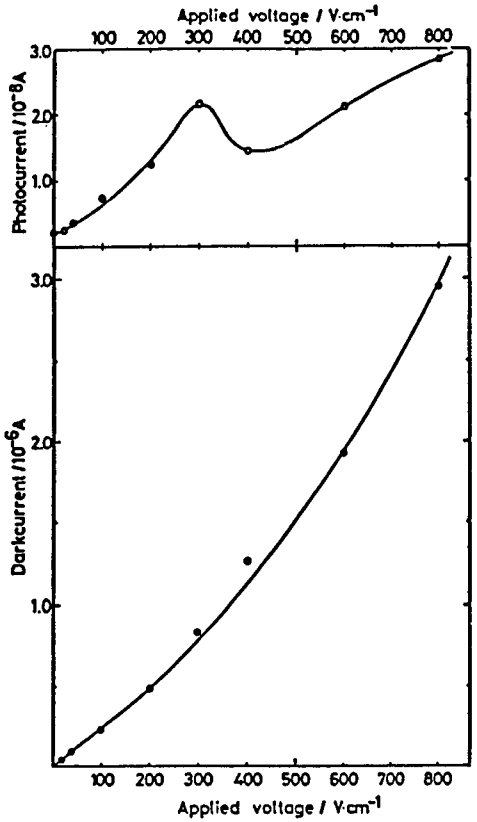

Figure 7 Current-voltage characteristics for a film of 2-(2-hydroxy-4-pentyloxy-benzylideneamino)-9-methylcarbazole(2e:n=5) in the isotropic liquid state(145°C). λ=400nm.

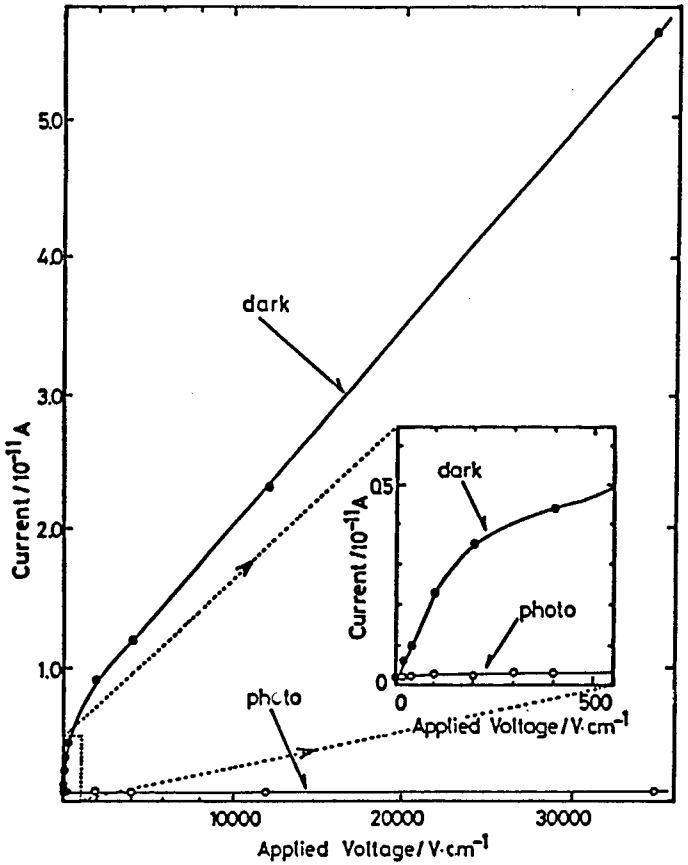

Figure 8 Current-voltage characteristics for a film of 2-(2-hydroxy-4-pentyloxybenzylidene-amino)-9-methylcarbazole(2e:n-5) in the crystalline state(28.5°C). λ=400nm.

might assist the charge carrier generation, it becomes more difficult for the carriers to move in a bulk region in the crystalline state than in the flow states. This seems to lead to the larger photocurrent in the flow states and to the large contribution of ionic carrier transport mechanism to the photocurrent. However, the electronic transport also seems to be contributed to the photocurrent, considering with the complex transport mechanism of liquid pyrene which consists of a mixture of ionic motion plus phonon-assisted electron transfers.[11]

It seems that the proposition by K.Okamoto et al.[2] could be applied to this case, meaning that the carrier species are ionic and that the negative carrier is O_2^- derived from oxygen molecules containing in the system and the positive carrier is cation radicals of 9-methylcarbazole liquid crystals. And the photoconducting behaviors in the nematic state resembles to those in the isotropic state rather than those in the crystalline state.

Conclusion

The photoconducting behaviors of 2-(2-hydroxy-4-pentyloxybenzylideneamino)-9-methylcarbazole(2e:n=5) were investigated and it was found that the behaviors in the nematic phase are similar to those in the isotropic liquid phase, both of them are fluid, rather than those in the crystalline phase.

The carrier transport mechanisms and the species are implied to follow the proposition by Okamoto et al.

The current-voltage characteristics strangely showed a new property in the flow states, being similar to that of the negative resistance as seen in a tunnel diode.

III—2 Photoconducting behaviors of 5,10,15,20-tetrakis(4-pentadecylphenyl)porphyrin through phase transitions

The SnO_2 sandwich cell of 5,10,15,20-tetrakis(4-pentadecylphenyl)porphyrin(4a:n=15) was not photoactive without bias.

Figure 9 shows the absorption and the action spectra for the films of 4a(n=15) in the crystalline state. 4000Vcm^{-1} of the field strength was applied for the action spectra.

For a 25μm-thick cell, the action spectrum appeared to be antibatic in relation to the absorption one, where the action one was red-shifted as compared with the absorption one and the photocurrent in the region where the absorption coefficient is

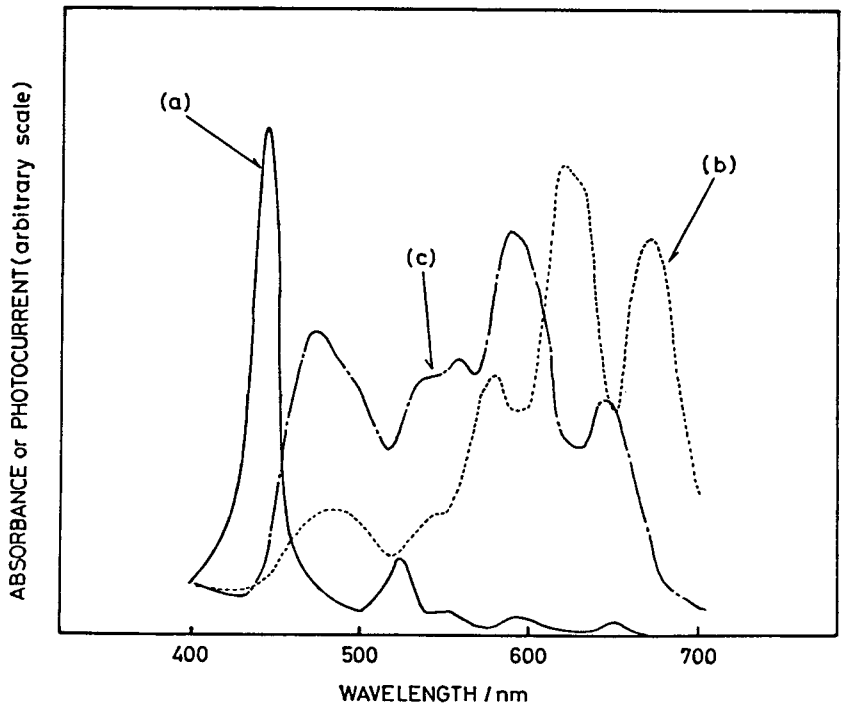

Figure 9 Action and absorption spectra for a film of 5,10,15,20-tetrakis(4-pentadecylphenyl)porphyrin(4a:n=15). (a)absorption, (b)25μm-thick cell and (c)6μm-thick cell in the crystalline phase(27°C). The action spectra are for the positive electrode illumination under 4000Vcm^{-1}.

larger, i.e. the Soret band, was rather smaller than that in the range with smaller absorption one, i.e. the Q band. For the 6μm-thick cell, however, the action spectra becomes coincident with the absorption spectrum in the range of the Q band and the degree of the red-shift becomes smaller for the two shorter wavelength bands of the Q band and the Soret one. Moreover, the photocurrent at about 470nm becomes relatively larger. These results indicate that the action spectra is dependent on the cell thickness. For a spin-coated film of which film thickness is estimated to be about 60nm, the action spectrum was found to be almost the same as the absorption spectra. Thus, it could be considered that the trapping sites and carrier recombination in the bulk region where the molecules no longer absorb the incident light, are contributed to the action spectra.

These cell-thickness dependence was also found for the light exponent σ, which is calculated by the relation of photocurrent to incident light intensity. Plots of them showed the good linearity as seen in Figure 10, typically. The light exponents σ for 6μm, 25μm and 50μm cells are calculated to be 0.66, 0.89 and 0.98, respectively. It was seen that the value of σ approaches to 0.5, as the cell-thickness decreases.

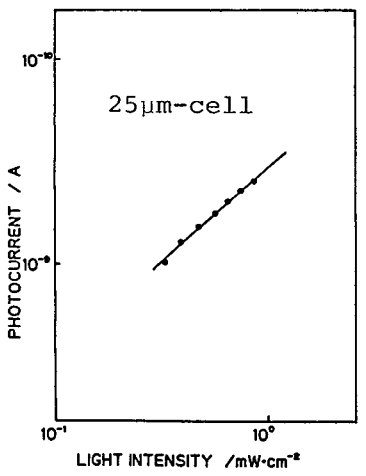

Figure 10 Plots of the photocurrent vs. incident light intensity of 620nm at 4000Vcm^{-1}.

These facts indicate that the charge-carrier generation

mechanism of 4a(n=15) in the crystalline state are complex.

Figure 11 showed the temperature dependence of the dark-current for 25μm-thick cell. In each phase, the behaviors were found to be of an Arrhenius type similar to those for rod-like liquid crystals. The activation energies for conduction ΔE are calculated to be 0.28, 0.69 and 0.30eV in the crystalline, m_1 and m_2 phases, respectively. The conductivities in each phase are in orders of 10^{-11}, 10^{-14}, 10^{-15} and less than 10^{-15}

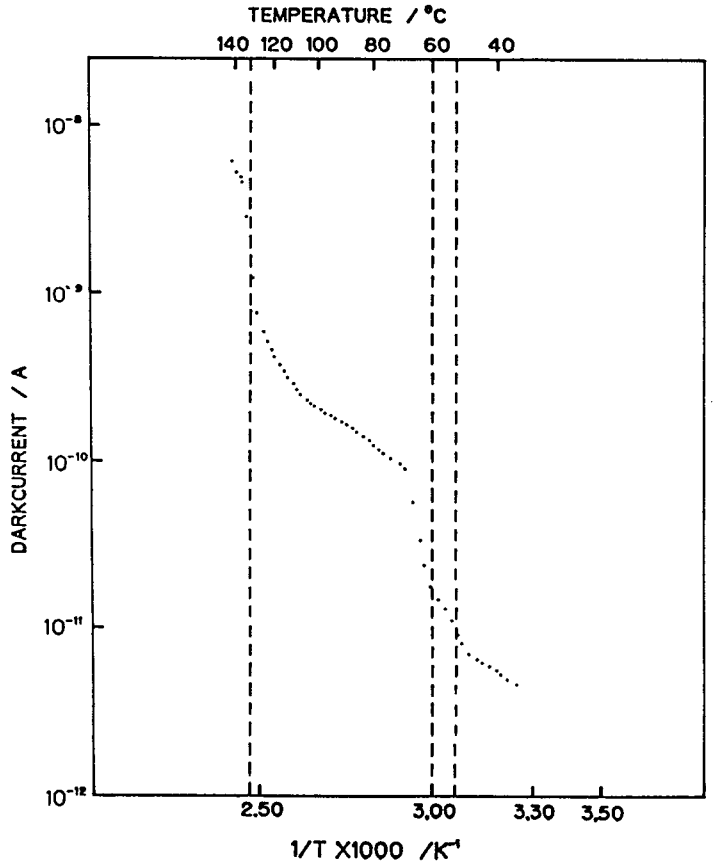

Figure 11 Temperature dependence of the darkcurrent for a 25μm-thick film of 5,10,15,20-tetrakis(4-pentadecylphenyl)porphyrin(4a:n=15) at 4000Vcm^{-1}.

Scm^{-1}. The darkcurrent abruptly increases at the m_1 to m_2 phase transition, as well as at the m_2 to isotropic liquid phase one.

On the other hand, the temperature dependence of the photocurrent shows different behaviors as shown in Figure 12. The photocurrent decreases as the temperature is elevated. This is the inverse situation against the behaviors for the darkcurrent. But the behaviors in each phase are apparently curious, that in the m_2 phase the photocurrent exhibits a minimum point and two maxima of the photocurrent are shown at the m_1 to m_2 and the m_2 to isotropic liquid phase transitions. These maxima seem to be due to the pretransitional phenomenon.

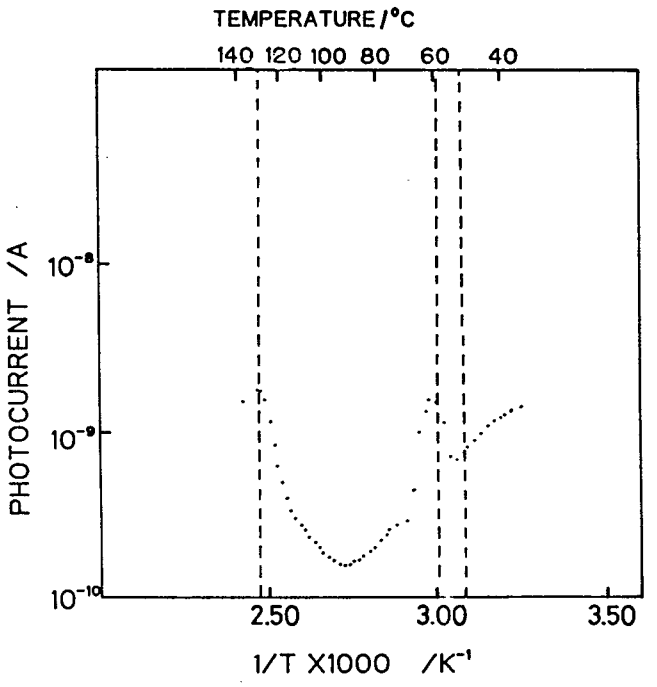

Figure 12 Temperature dependence of the photocurrent for a 25μm-thick film of 5,10,15,20-tetrakis(4-pentadecylphenyl)porphyrin(4a:n=15) at $4000Vcm^{-1}$ in the positive electrode illumination. The wavelength of incident light is 620nm.

These facts indicate that the carrier transport processes in the crystal, m_1 and m_2 phases are not ionic one, but electronic, as having been considered to be[12], since if the transport process is ionic, the photocurrent should increase at the m_2 to isotropic phase transition as seen in the case of a rod-like 9-methylcarbazole liquid crystal.

The carrier generation mechanism of 5,10,15,20-tetraphenylporphyrin is considered to be of extrinsic one in the presence of recombination.[7] In the present case, however, the cell is of sandwich type and the interface between coated SnO_2 and porphyrin molecules are not photoactive. Moreover, the rectification of the darkcurrent was not shown in the darkcurrent-voltage characteristic, leading to the non-Schottky interface. Thus, the intrinsic process seems to be contributed to the photocurrent in some extent.

Figure 13 shows the temperature dependence of the ratio i_p/i_d, in which i_p and i_d are photo- and dark-current, respectively. The ratio was found to change from 300 at 35°c to 0.25 at 140°C through the phase transitions. At the m_2 to isotropic liquid and the m_1 to m_2 phase transitions, the ratio was shown to abruptly decrease.

These temperature dependences indicate that the phase transitions of 4a(n=15) could influence the photoconducting behaviors in large extent.

Conclusion

The photoconducting behaviors of 5,10,15,20-tetrakis(4-pentadecylphenyl)porphyrin(4a:n=15) accompanying several phase transition between crystalline and isotropic liquid phases,

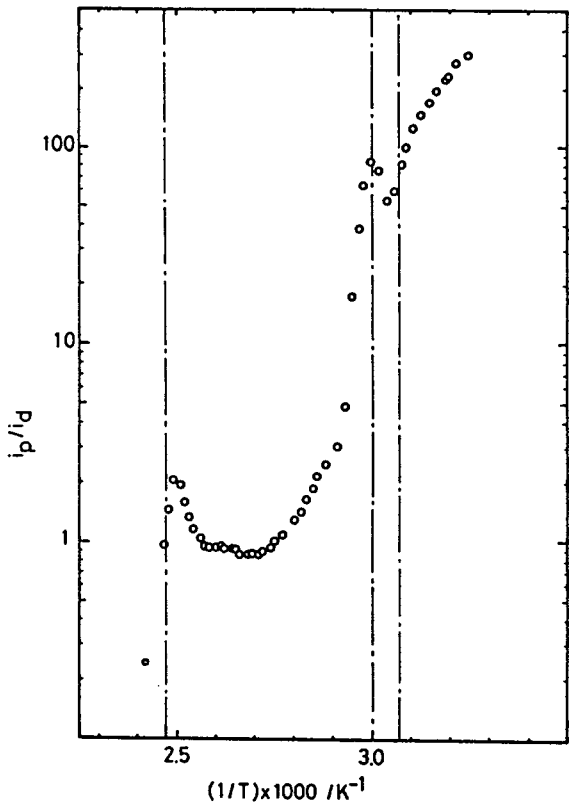

Figure 13 Temperature dependence of the ratio i_p/i_d for a 25μm-thick film of 5,10,15,20-tetrakis(4-pentadecylphenyl)porphyrin(4a:n=15). The ratios were calculated from the results of Figures 11 and 12.

were investigated and large gaps of the i_p/i_d at the phase transitions of the m_1 to m_2 and the m_2 to isotropic phases were found. Considering the electronic carrier transport process, the state of the m_2 phase seems to depress the carrier transport due to the enlargement of the molecular separation and the molecular fluctuation.

REFERENCES

1) S.Kusabayashi and M.M.Labes, Mol.Cryst.Liq.Cryst., 7, 395 (1969).

2) K.Okamoto, S.Nakajima, A.Itaya and S.Kusabayashi, Bull.Chem. Soc.Jpn., 56, 3545(1983).

3) K.Okamoto, S.Nakajima, M.Ueda, A.Itaya and S.Kusabayashi, Bull.Chem.Soc.Jpn., 56, 3830(1983).

4) M.Yokoyama, Y.Endo and H.Mikawa, Chem.Phys.Lett., 34, 597 (1975);M.Yokoyama, Y.Endo and H.Mikawa, Bull.Chem.Soc.Jpn., 49, 1538(1976).

5) K.Okamoto, N.Oda, A.Itaya and S.Kusabayashi, Chem.Phys.Lett., 35, 483(1975).

6) L.L.Chapoy, D.K.Munck, K.H.Rasmussen, E.Juul Diekmann, R.K. Sethi and D.Biddle, Mol.Cryst.Liq.Cryst., 105, 353(1984).

7) K.Yamashita, K.Maenobe and J.Fajer, Chem.Lett., 307(1980).

8) R.F.Chaiken and D.R.Kearns, J.Chem.Phys., 45, 3966(1966).

9) L.Esaki and P.J.Stiles, Phys.Rev.Lett., 16, 1108(1966).

10) E.F.Carr, Mol.Cryst., 7, 253(1969);W.J.Helfrich, J.Chem.Phys., 51, 4092(1969).

11) O.H.LeBlanc,Jr., J.Chem.Phys., 37, 916(1962).

12) K.Yamashita, N.Kihara, H.Shimidzu and H.Suzuki, Photochem. Photobiol., 35, 1(1982) and references cited therein.

Acknowledgment

The author would like to express sincerest gratitude to Professor Shigekazu Kusabayashi at Faculty of Engineering, Osaka University for his continuous guidance and hearty encouragement throughout this work.

The author is deeply indebt to Lecturer Masatomo Nojima, whose advice, encouragement and influence have been essential in the accomplishment of this study. The author is also grateful to Associate Professor Yasuhiko Kondo and Lecturer Shunsuke Takenaka for their advices.

Associate Professor Masaaki Yokoyama has given the author a lot of useful suggestions in this work and he would like to acknowledge him sincerely.

The author acknowledges Professor Hikaru Terauchi at Department of Physics, Kwansei-Gakuin University and his collaborators, Yasuo Nishihata and Kazuya Kamon for their collaborations in the X-ray diffraction study.

The author further wishes to thank Dr. Masato Takagi and Dr. Masahiro Miura. Their warmhearted advices have encouraged him in this work. His acknowledgment is also offered to Atsushi Ishikawa, a student in the master course for his collaborations. Furthermore, the author wishes to thank all the members of the Kusabayashi Laboratory for their friendships.

Finally, the author would like to thank his father, Dr. Kazuhiro Shimizu and his mother, Eiko Shimizu for their understanding and perpetual support.